Electronic Supporting Information (ESI)

Fully bio-derived CO_2 polymers for non-isocyanate based polyurethane synthesis

S.-E. Dechent[a], A. W. Kleij,[b,c,*] G. A Luinstra[a,*]

[a] University of Hamburg, Institute for Technical and Macromolecular Chemistry, Bundesstr. 45, 20146 Hamburg, Germany

[b] Institute of Chemical Research of Catalonia (ICIQ), The Barcelona Institute of Science and Technology (BIST), Av. Països Catalans 16, 43007 − Tarragona, Spain

[c] Catalan Institute of Research and Advanced Studies (ICREA), Pg. Lluís Companys 23, 08010 – Barcelona, Spain

E-mail: akleij@iciq.es; luinstra@chemie.uni-hamburg.de

Contents

1. Characterization of PBDs

1.1 Summarized properties of PBD1 - PBD4

Table S1. Detailed properties of PBD1 - PBD4.

polymer	M_n [kg/mol][a]	Đ[a]	double bond units [%][b]				double bond units [%][c]		double bonds [mmol/g][d]	T_g (°C)[e]	T_d (°C)[f]
			1,4-		1,2-		1,4-	1,2-			
			cis	trans	cyclic	vinyl	cis/-trans	cyclic/-vinyl			
PBD1	1.14	2.33	40.8		30.1	29.1	40.7	59.3	11.7	- 56	249
PBD2	2.63	2.58	44.4	36.6	1.1	18.9	81.4	18.6	16.0	- 94	347
PBD3	11.0	1.12	42.1	44.0	0.4	13.5	88.1	11.9	16.7	- 94	351
PBD4	39.4	1.12	45.8	43.9	0.2	10.2	91.6	8.40	14.2	- 99	365

[a]Measured by GPC (THF, RT) using polystyrene standards. [b]Determined by ^{1}H NMR analysis using normalized proton areas (A): $X_{double\ bond\ type}(\%) = \frac{A_{double\ bond\ type}}{A_{total}} \cdot 100$. [c]Determined by ^{13}C igated NMR analysis using normalized carbon areas (A): $X_{1,4-cis/-trans}(\%) = \frac{A_{1,4-cis/-trans} - A_{styrene}}{A_{total-}\ A_{styrene}} \cdot 100$ and $X_{1,2-cylic/-vinyl}(\%) = \frac{A_{1,2-cyclic/-vinyl,=CH_2}}{A_{total-}\ A_{styrene}} \cdot 100.$ [d]Measured by epoxide titration (see Supporting Information Section 3). [e]Determined by DSC; data are taken from the second heating. [f]Decomposition temperature (T_d) determined by TGA at 1% weight loss.

1.2 Spectroscopic analysis

1.2.1 PBD1

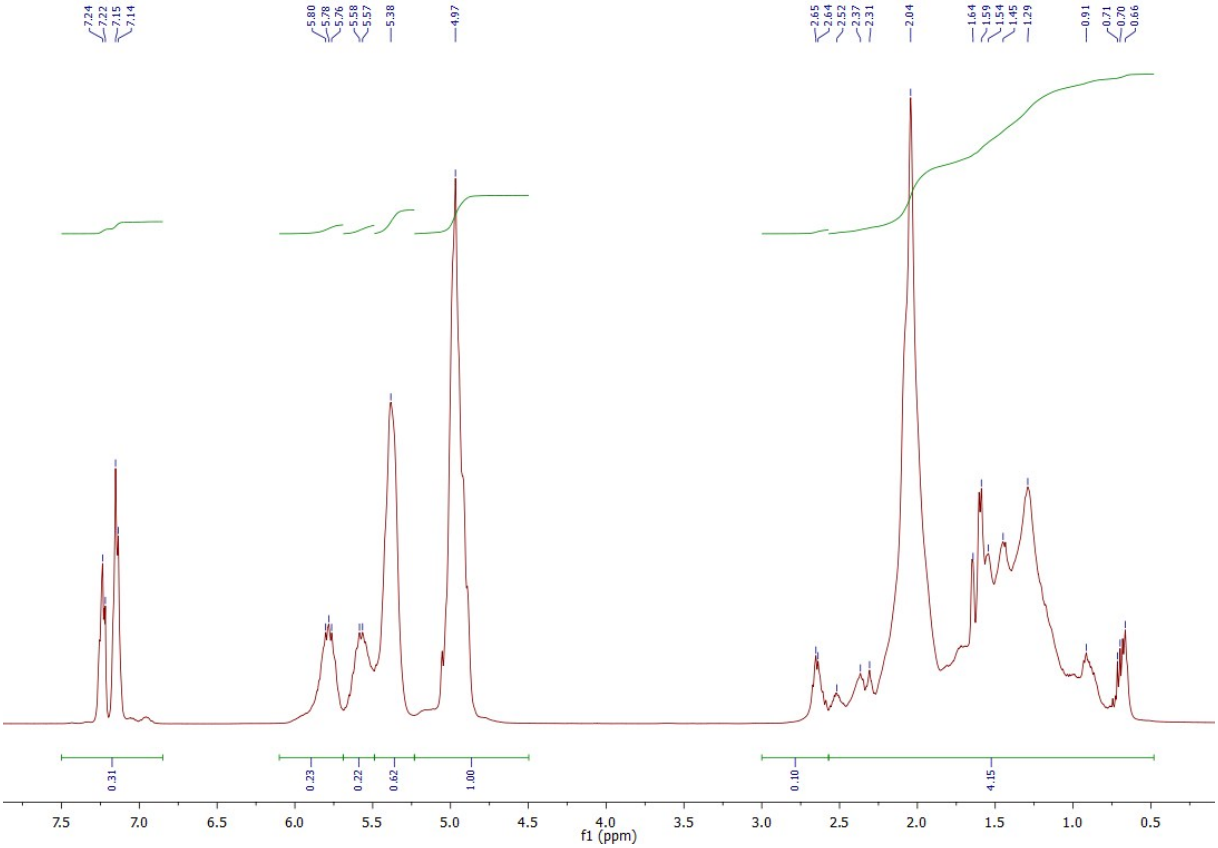

Figure S1. ^{1}H NMR spectrum of **PBD1** in $CDCl_3$ (Table S1).

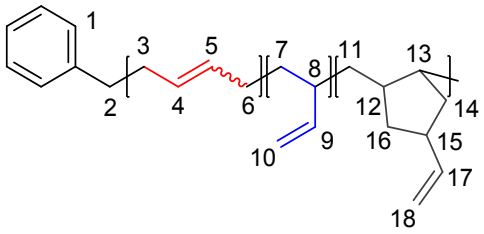

^{1}H NMR ($CDCl_3$, 400 MHz): δ (ppm) = 7.50-6.85 (m, 5H, 1-CH),6.1-5.69 (m, 1H, 17-CH), 5.69-5.49 (m, 1H, 9-CH), 5.49-5.23 (m, 2H, 4-CH, 5-CH), 5.23-4.50 (m, 2H, 10-CH_2, 18-CH_2), 3.00-2.57 (m, 2H, 2x2-CH), 2.57-0.48 (m, 16H, 2x3-CH, 2x6-CH, 2x7-CH, 8-CH, 2x11-CH, 12-CH, 13-CH, 2x14-CH, 15-CH, 2x16-CH).

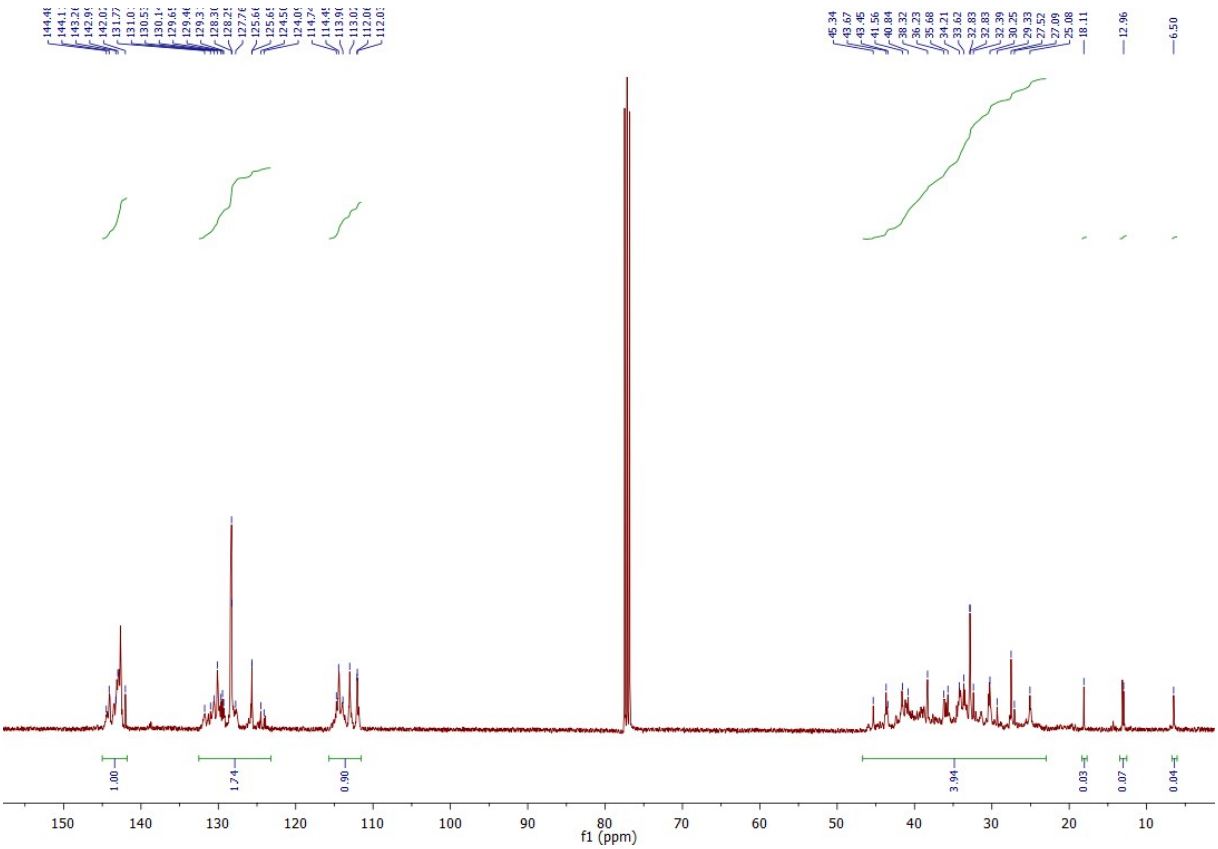

Figure S2. ^{13}C NMR spectrum of **PBD1** in $CDCl_3$ (Table S1).

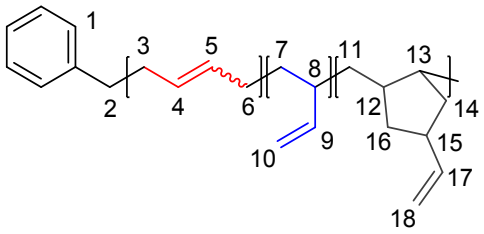

^{13}C NMR ($CDCl_3$, 125 MHz): δ (ppm) = 145.0-141.8 (1x1-C (styrene end group), 9-C, 17-C), 132.5-123.2 (5x1-C (styrene end group), 4-C, 5-C), 115.7-111.5 (10-C, 18-C), 46.7-6.05 (2-C, 3-C, 6-C, 7-C, 8-C, 11-C, 12-C, 13-C, 14-C, 15-C, 16-C).

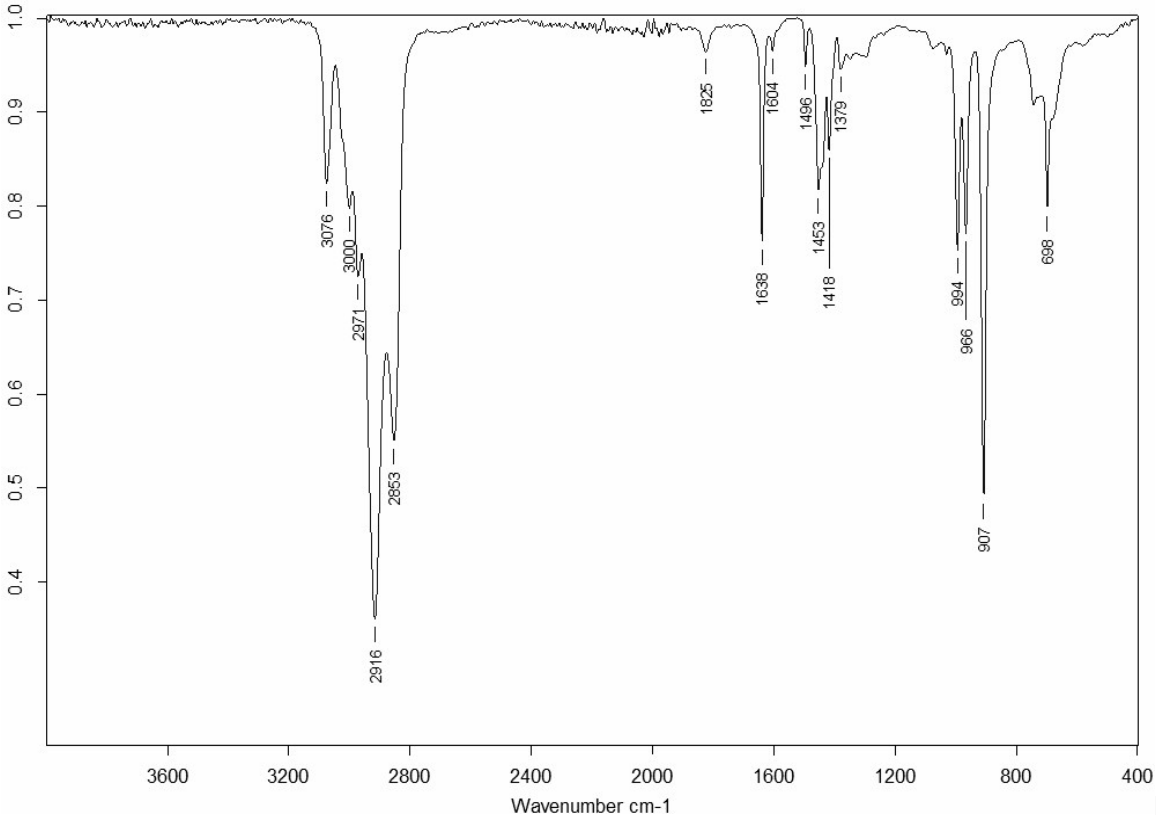

Figure S3. IR spectrum of **PBD1** (Table S1).

1.2.2 PBD2

Please note the peak assignments in Figure S1 and S2. The signal for 1, 4-cis and 1,4-trans double bonds splits into the signals at *δ* (ppm) = 5.42 (m, 2H (trans)) and 5.38 (m, 2H, (cis)).

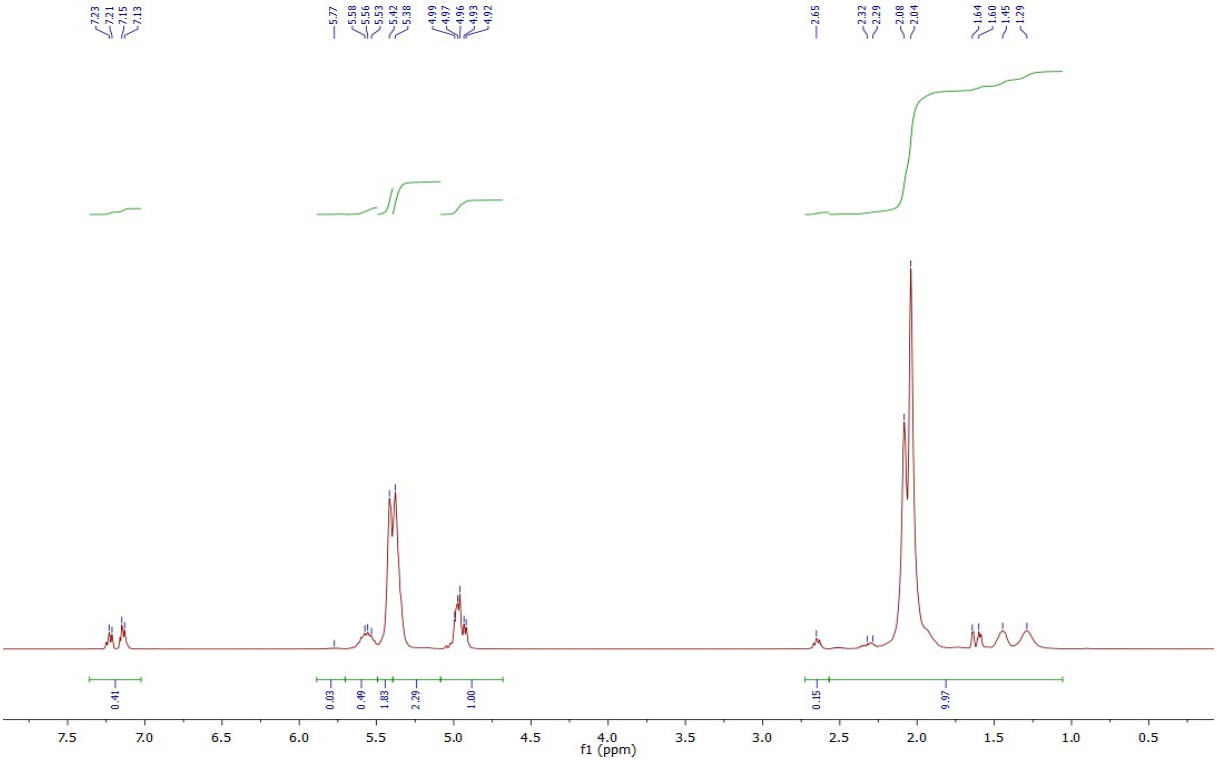

Figure S4. ^{1}H NMR spectrum of **PBD2** in $CDCl_3$ (Table S1).

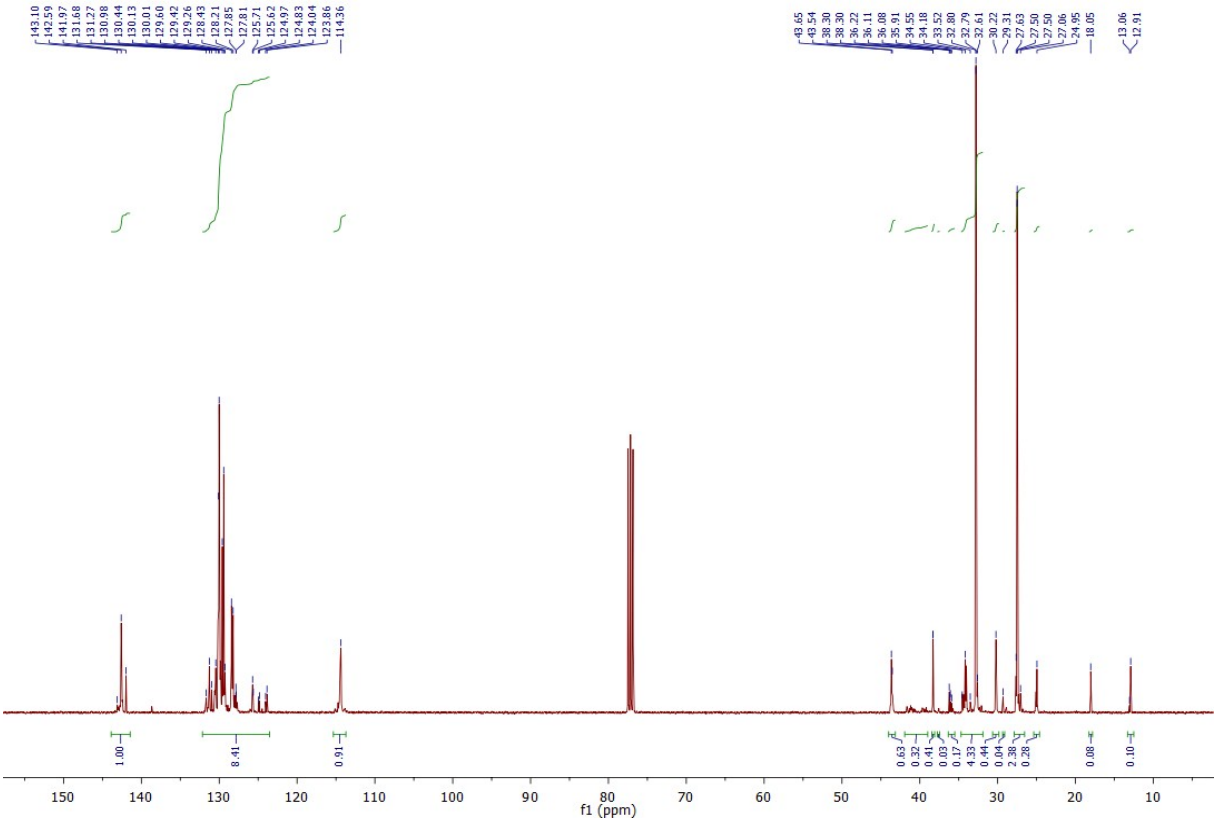

Figure S5. ^{13}C NMR spectrum of **PBD2** in $CDCl_3$ (Table S1).

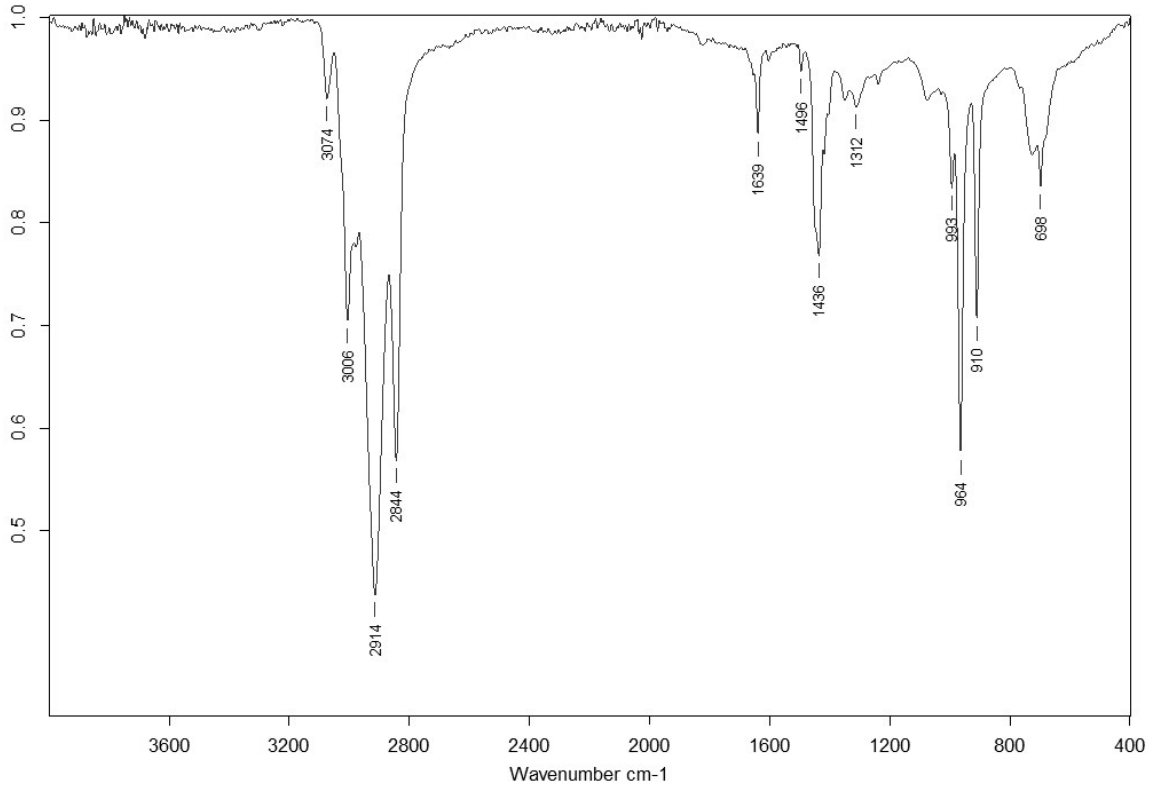

Figure S6. IR spectrum of **PBD2** (Table S1).

1.2.3 PBD3

Please note the peak assignments in Figure S1 and S2. The signal for 1,4-cis and 1,4-trans double bonds splits into the signals at *δ* (ppm) = 5.46 (m, 2H (trans)) and 5.41 (m, 2H, (cis)).

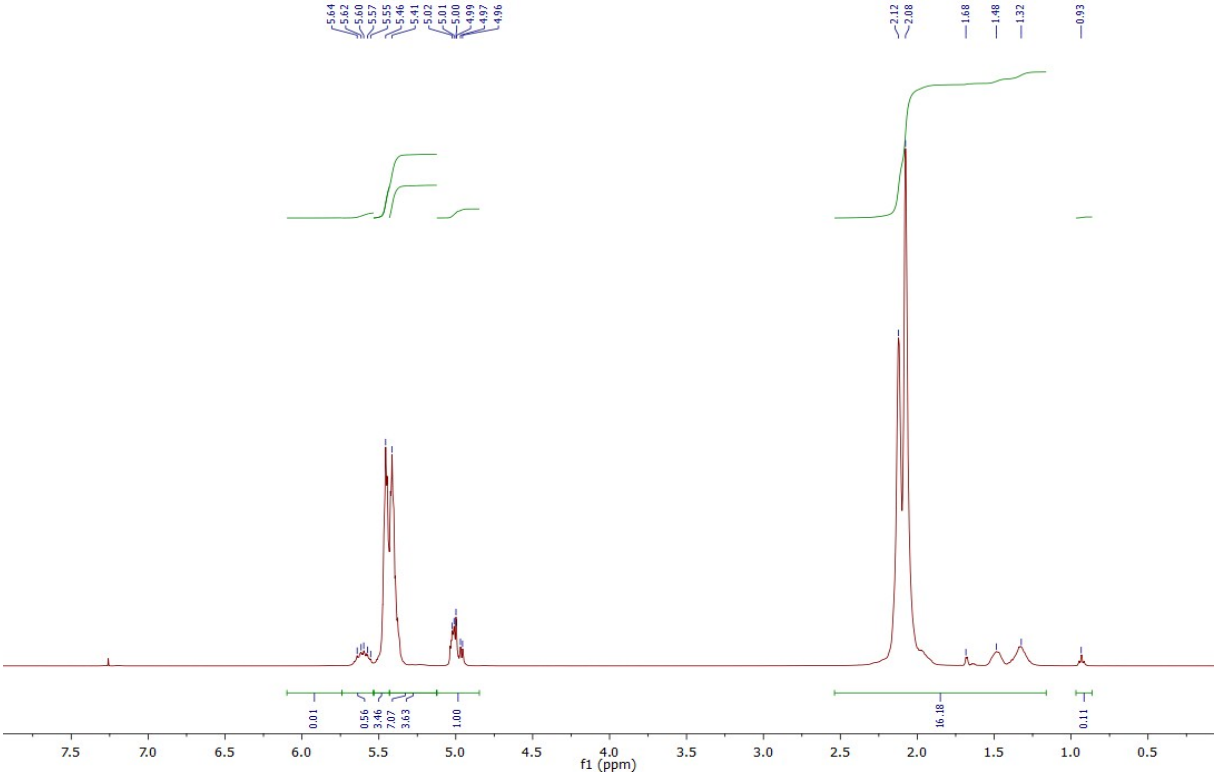

Figure S7. ^{1}H NMR spectrum of **PBD3** in $CDCl_3$ (Table S1).

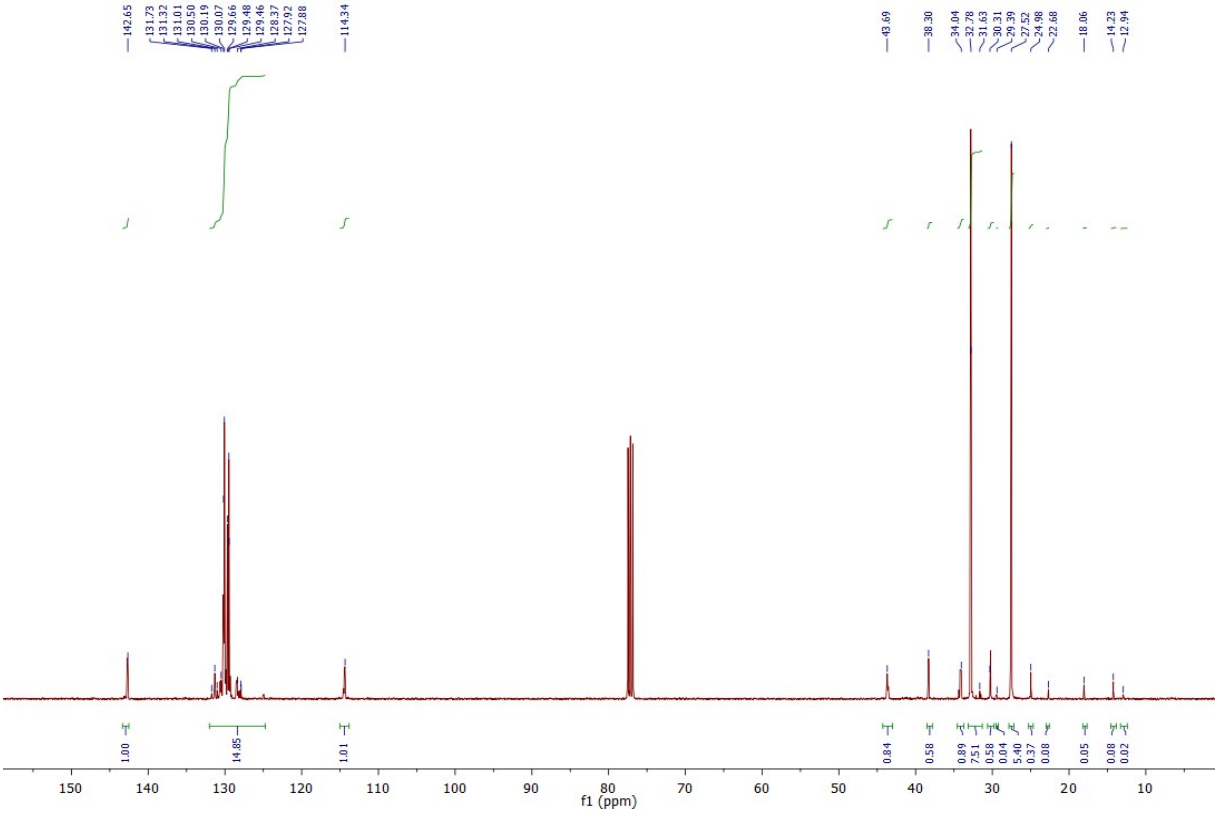

Figure S8. ^{13}C NMR spectrum of **PBD3** in $CDCl_3$ (Table S1).

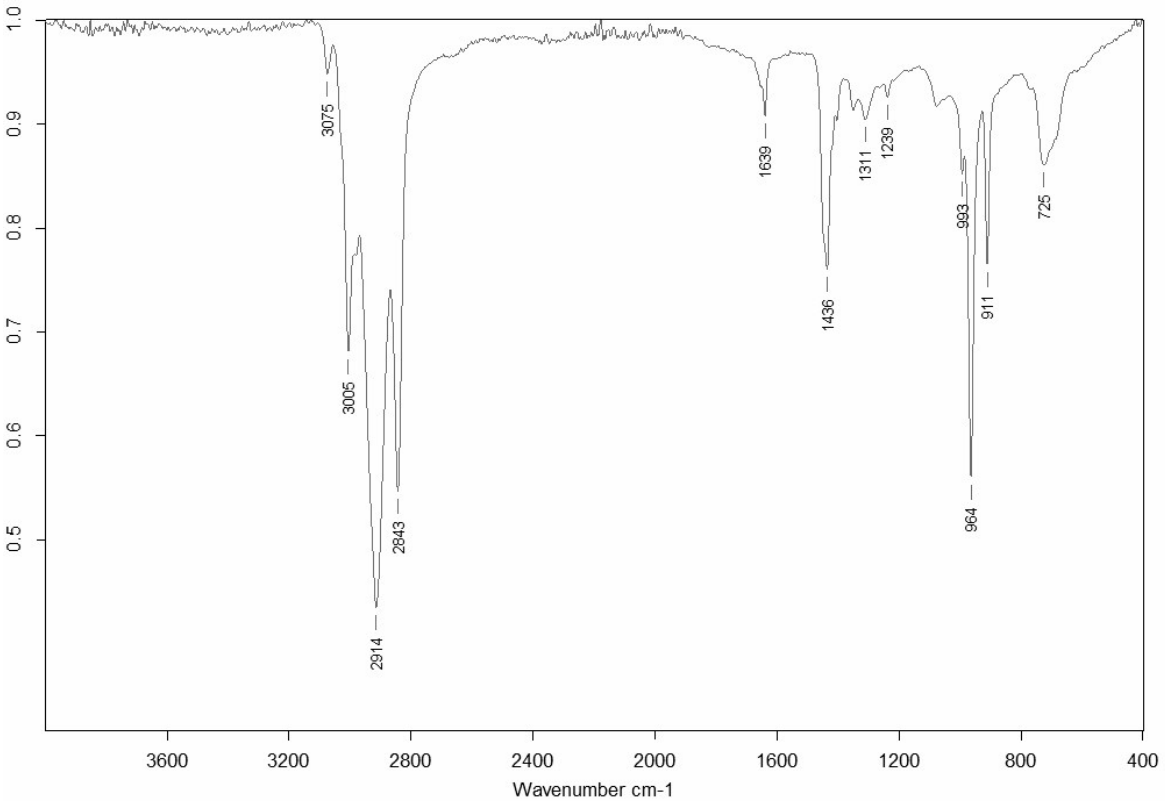

Figure S9. IR spectrum of **PBD3** (Table S1).

1.2.4 PBD4

Please note the peak assignments in Figure S1 and S2. The signal for 1, 4-cis and 1, 4-trans double bonds splits into the signals at *δ* (ppm) = 5.45 (m, 2H (trans)) and 5.40 (m, 2H, (cis)).

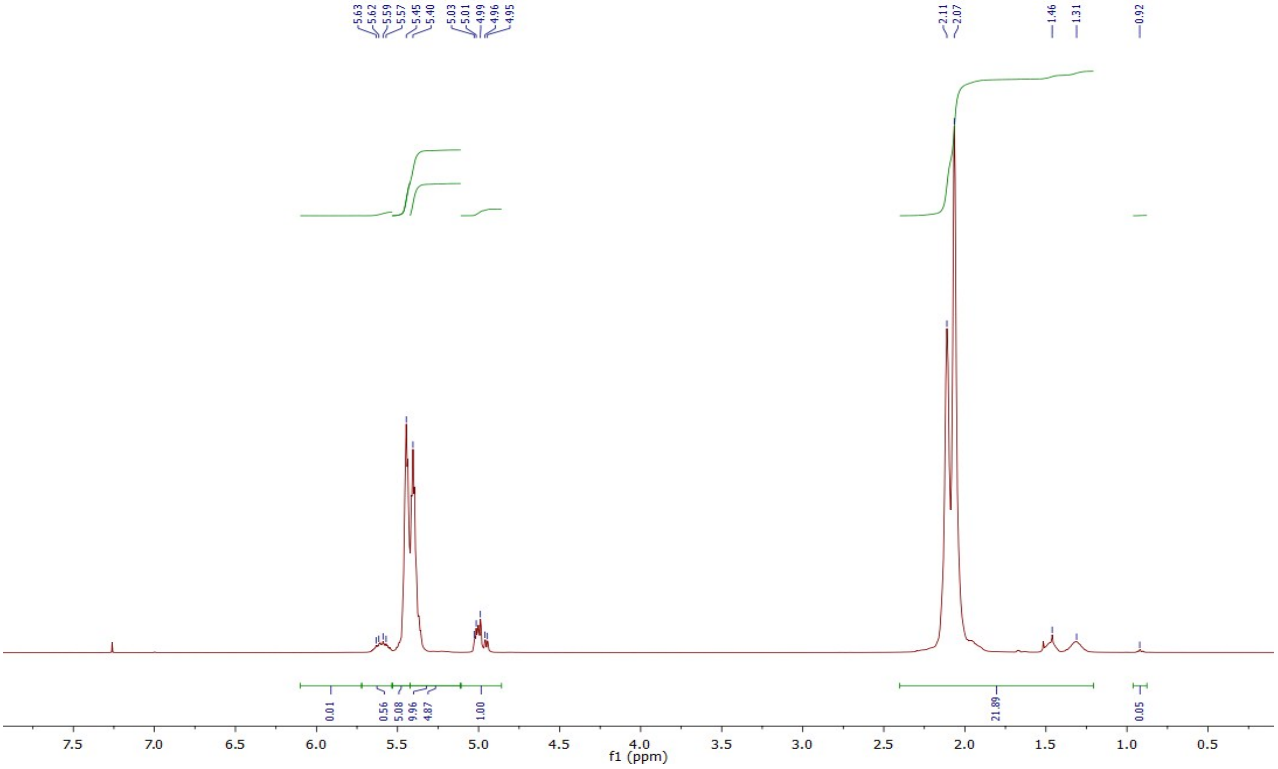

Figure S10. ^{1}H NMR spectrum of **PBD4** in $CDCl_3$ (Table S1).

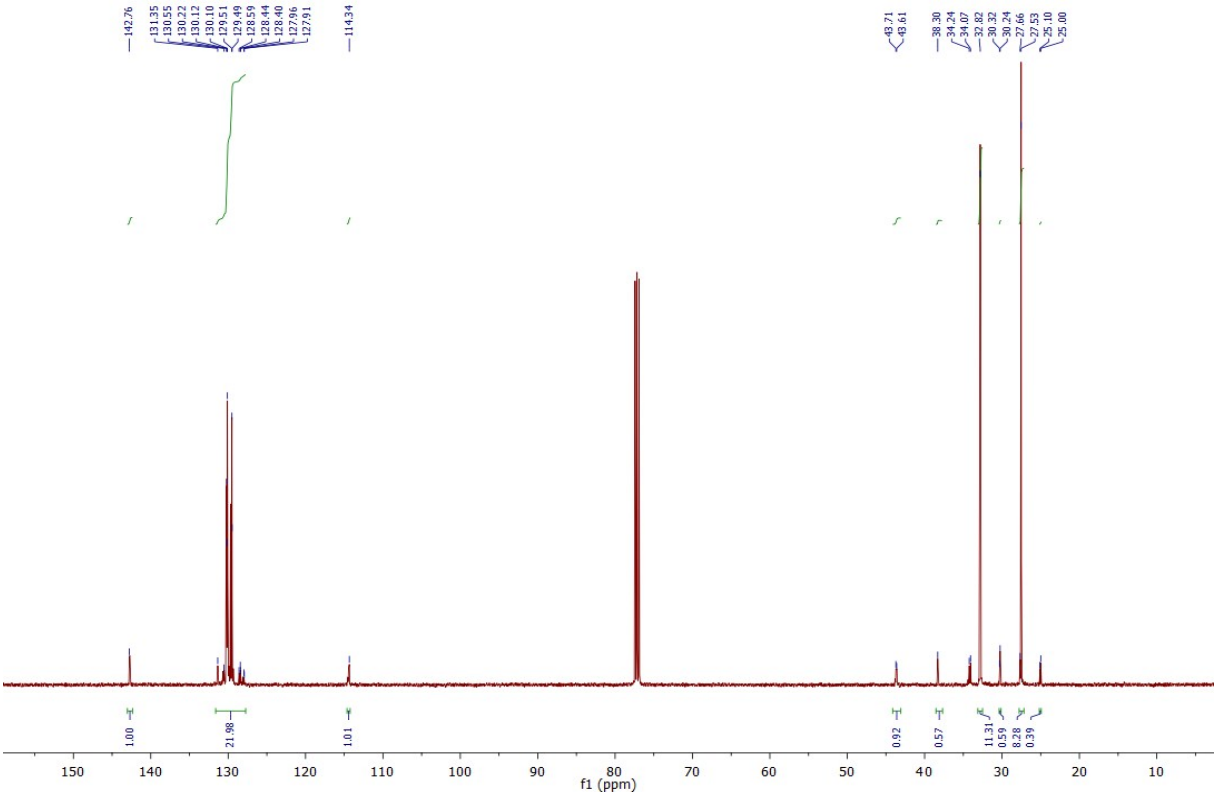

Figure S11. ^{13}C NMR spectrum of **PBD4** in $CDCl_3$ (Table S1).

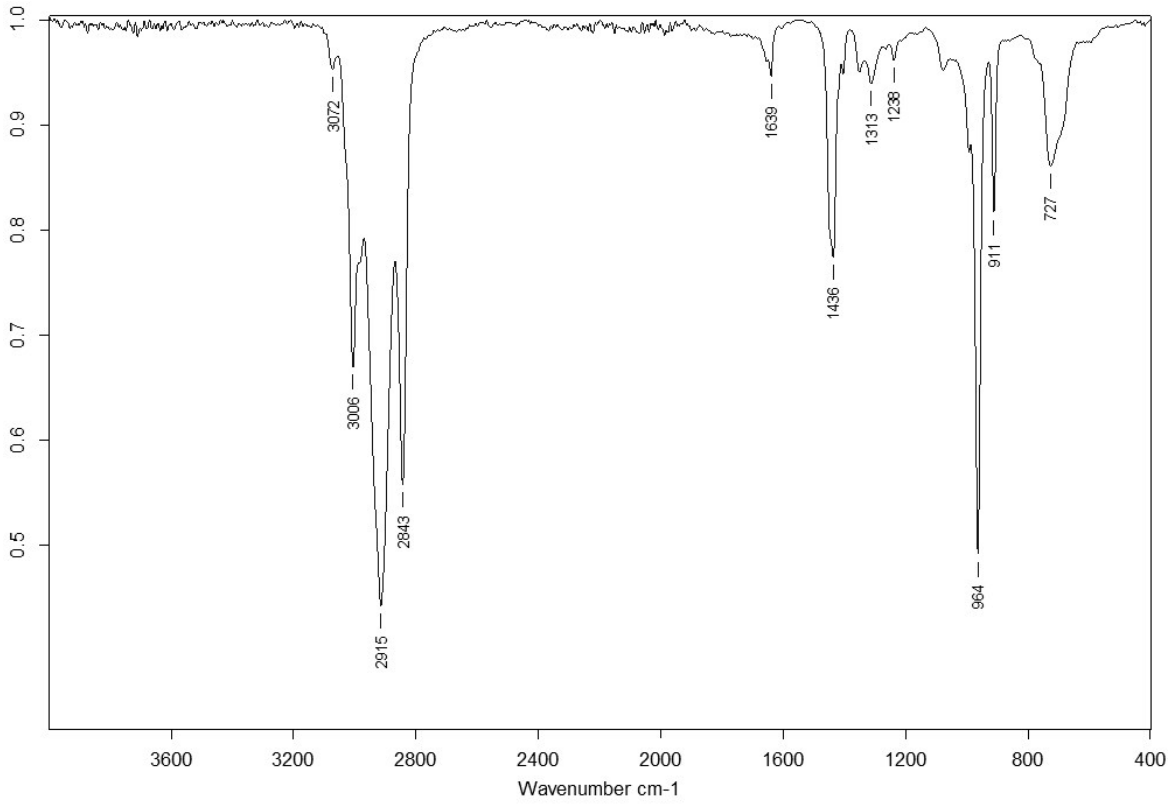

Figure S12. IR spectrum of **PBD4** (Table S1).

1.3 Thermal analysis

1.3.1 PBD1

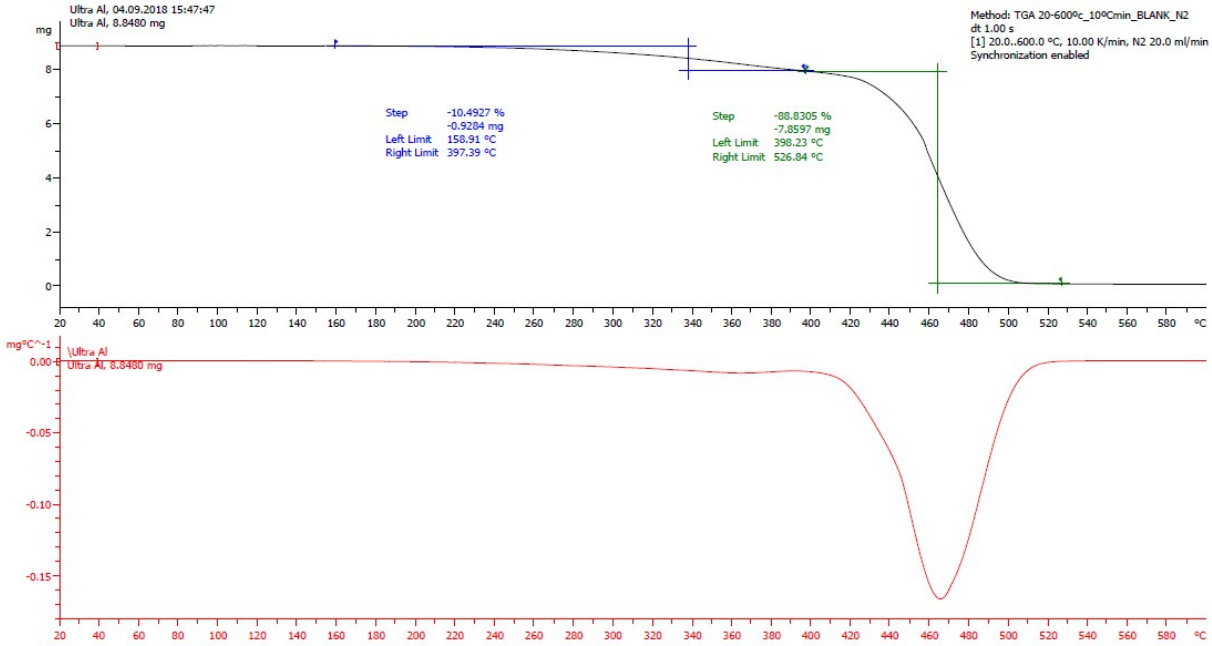

Figure S13. Thermogravimetric analysis of **PBD1** (Table S1).

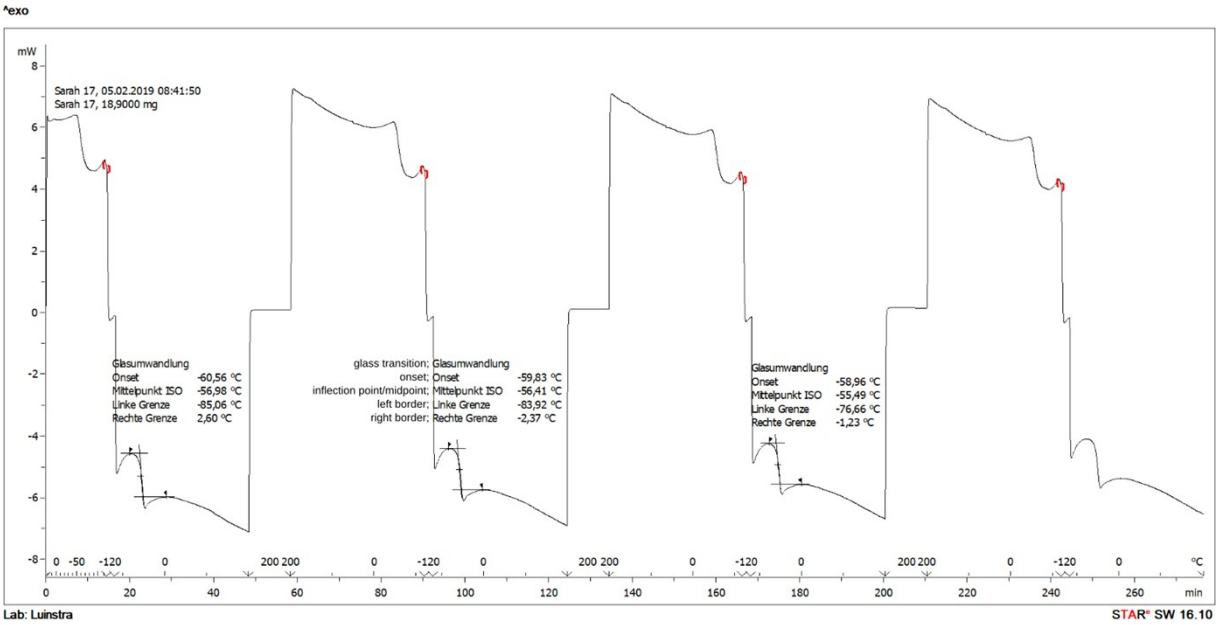

Figure S14. Differential Scanning Calorimetry trace of **PBD1** (Table S1).

1.3.2 PBD2

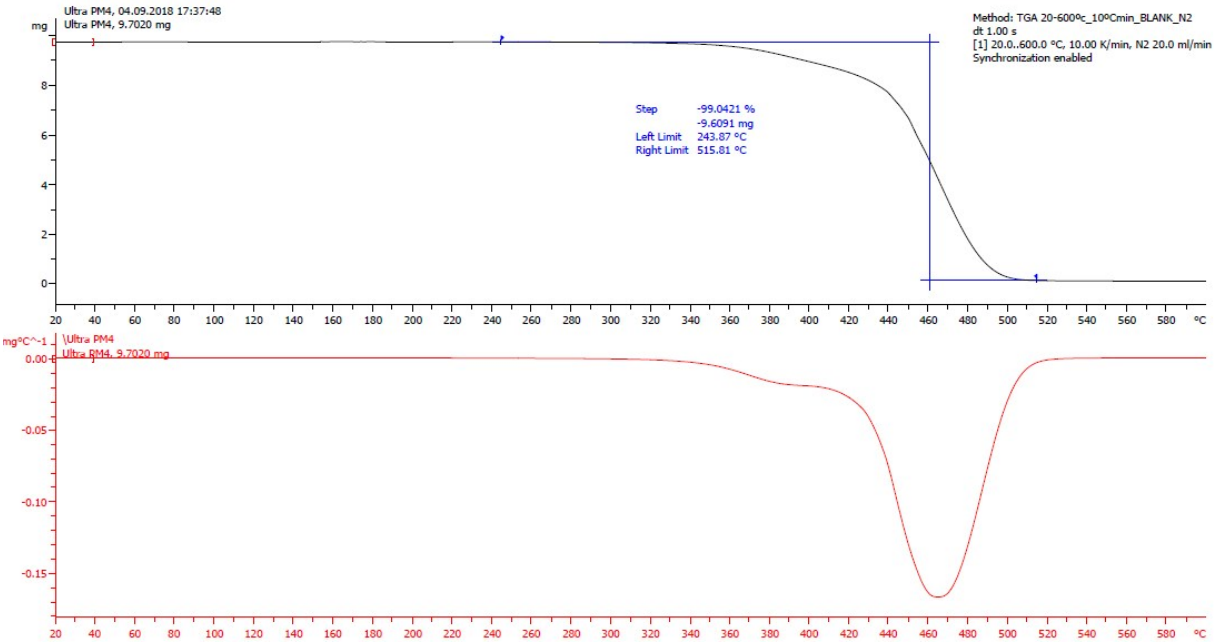

Figure S15. Thermogravimetric analysis of **PBD2** (Table S1).

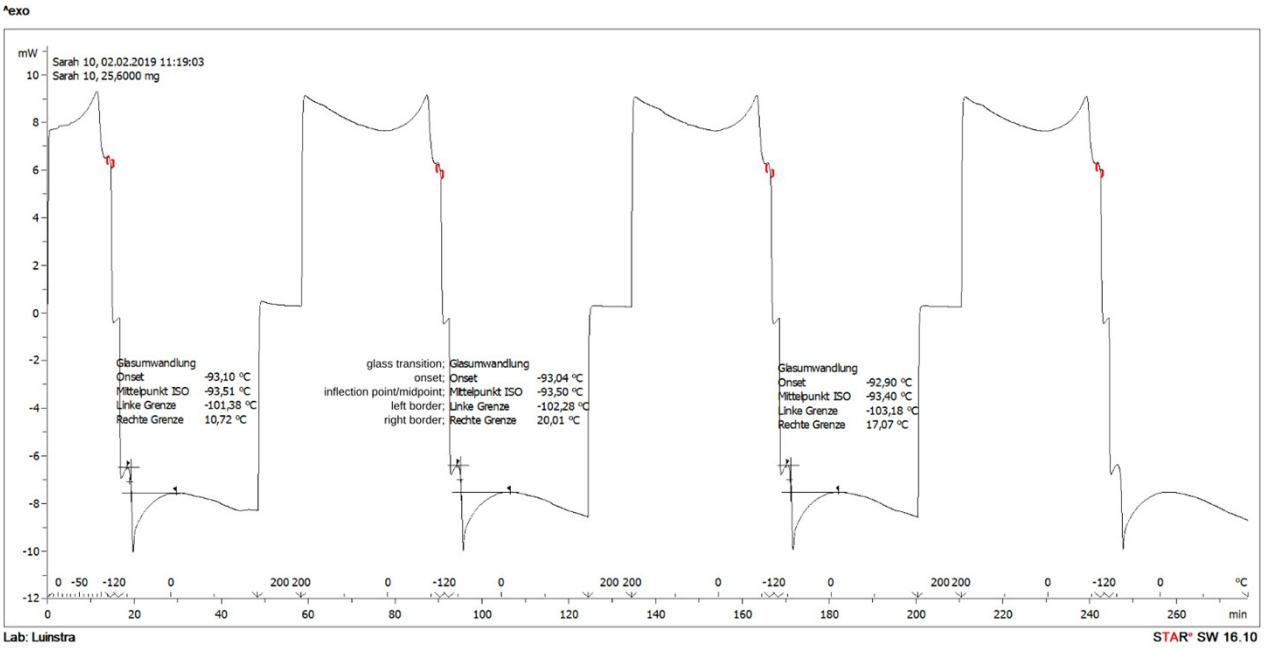

Figure S16. Differential Scanning Calorimetry trace of **PBD2** (Table S1).

1.3.3 PBD3

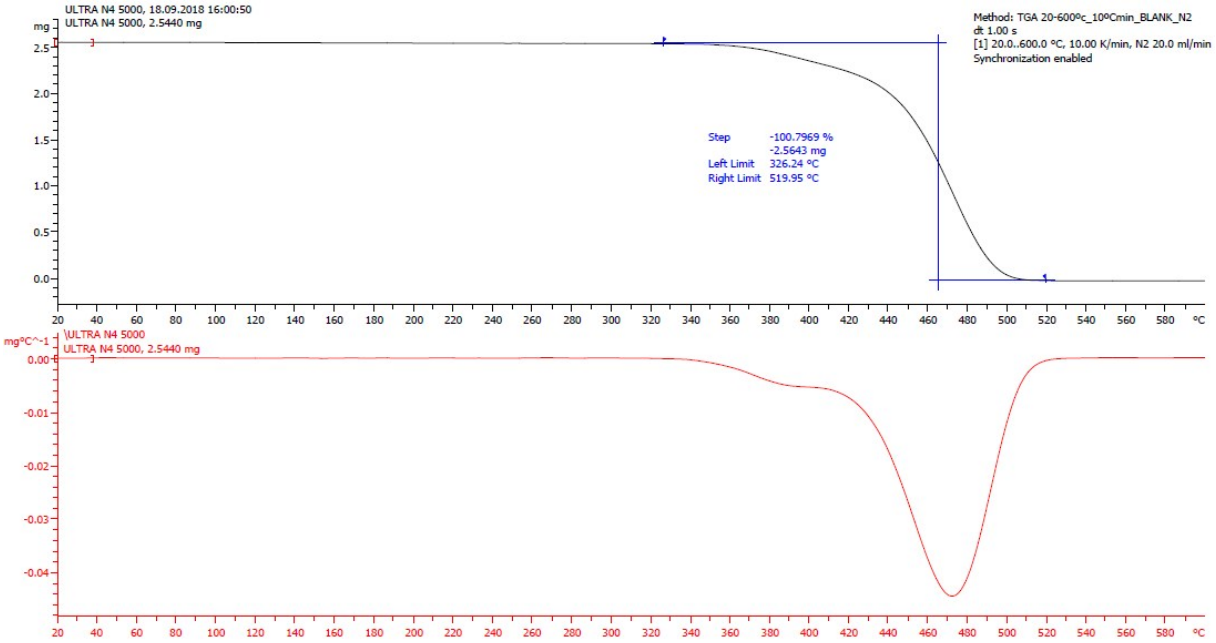

Figure S17. Thermogravimetric analysis of **PBD3** (Table S1).

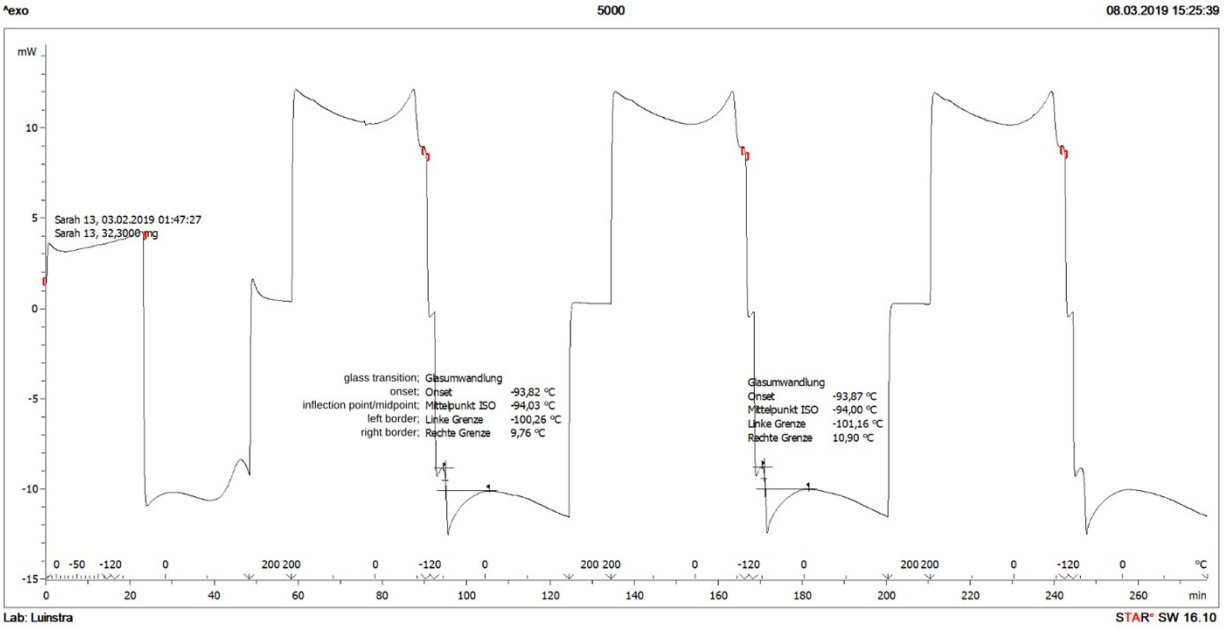

Figure S18. Differential Scanning Calorimetry trace of **PBD3** (Table S1).

1.3.4 PBD4

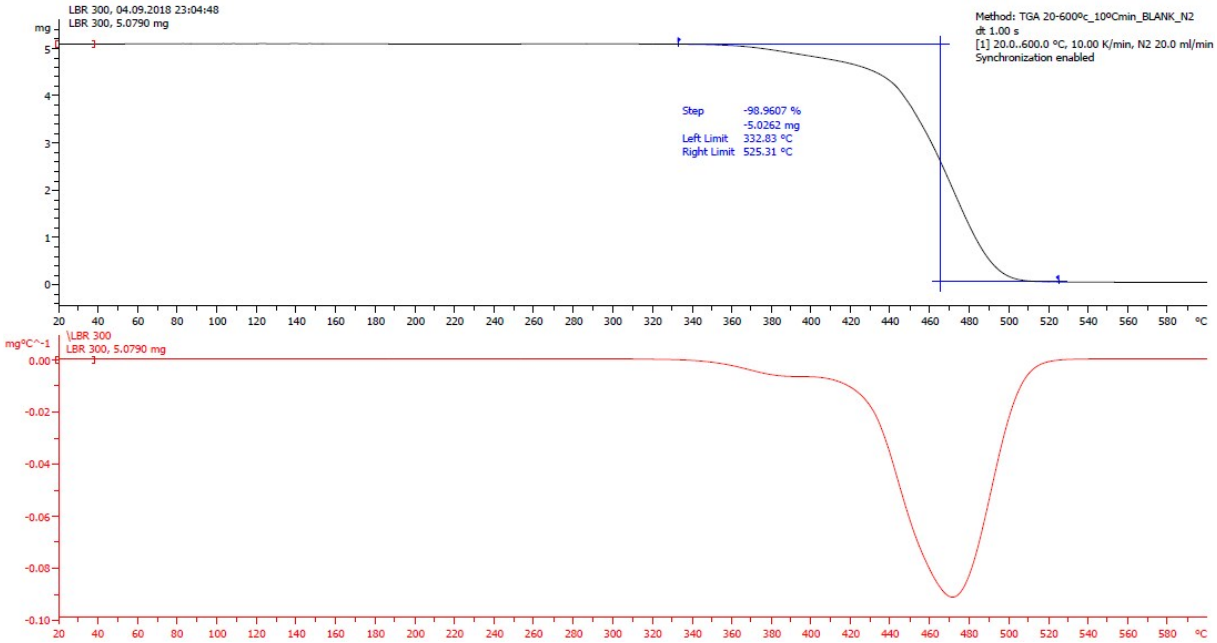

Figure S19. Thermogravimetric analysis of **PBD4** (Table S1).

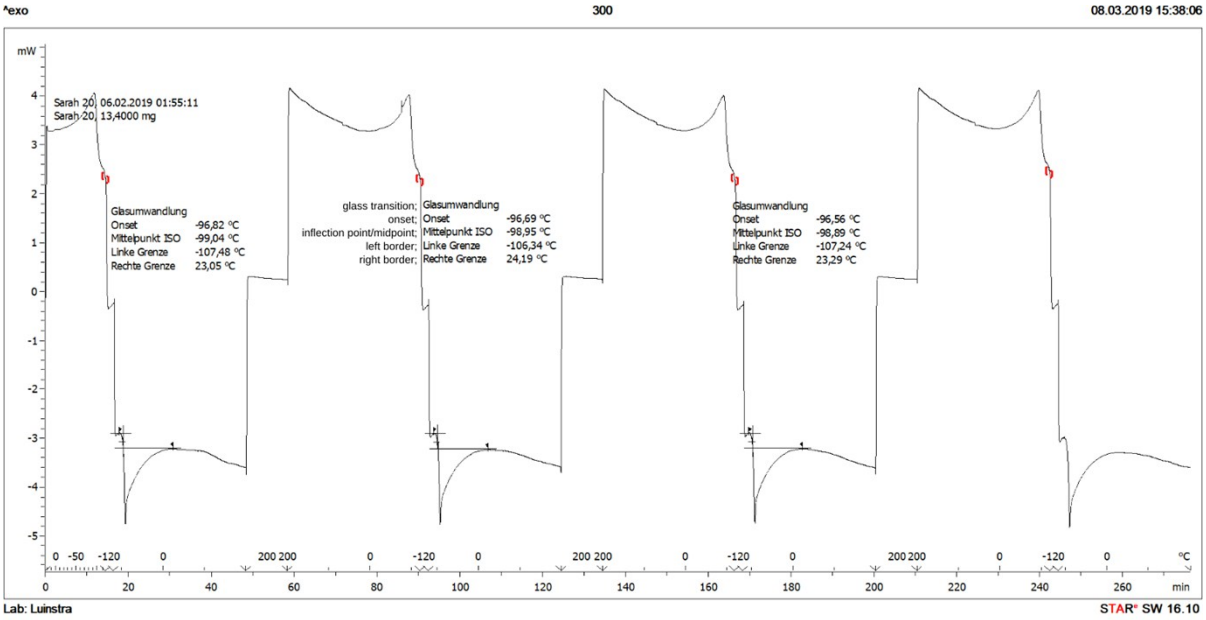

Figure S20. Differential Scanning Calorimetry trace of **PBD4** (Table S1).

2. Characterization of PE-PBDs

2.1 Summarized properties of PE-PBD1 - PE-PBD4

Table S2. Detailed properties of PE-PBD1 - PE-PBD4.

polymer	M_n [kg/mol][a]	Đ[a]	epoxide units [%]				EP-number[d] [mmol/g]	T_g (°C)[e]	T_d (°C)[f]
			total	1, 4-[b]		1,2-[b]			
				trans	cis	cyclic/-vinyl			
PE-PBD1	1.10	2.43	13.9[b] 10.9[c]	6.50	5.95	1.47	1.62	- 45	259
PE-PBD2	2.64	2.56	8.26[b] 7.20[c]	3.85	4.02	0.39	1.33	- 87	322
PE-PBD3	11.5	1.16	11.8[b] 11.2[c]	5.74	5.95	0.07	1.96	- 83	362
PE-PBD4	39.7	1.13	10.7[b] 9.70[c]	5.13	5.32	0.20	1.51	- 88	375

[a]Measured by GPC (THF, RT) using polystyrene standards. [b]Determined by ^{1}H NMR analysis using normalised proton areas for epoxide and double bonds: $X_{1,2-cyclic/-vinyl\ epoxide}\ or\ X_{1,4-cis\ epoxide}(\%) = \frac{A_{epoxide\ type}}{A_{total} - A_{methylene\ group,\ styrene}} \cdot 100$ and $X_{1,4-trans\ epoxide}(\%) = \frac{A_{epoxide\ type} - A_{methylene\ group,\ styrene}}{A_{total} - A_{methylene\ group,\ styrene}} \cdot 100$. [c]Determined by ^{13}C igated NMR analysis using normalized carbon areas of epoxides and double bonds: $X_{epoxide}(\%) = \frac{A_{epoxide}}{A_{total} - A_{styrene}} \cdot 100$. [d]Measured by epoxide titration (see Supporting Information Section 3). [e]Determined by DSC; data are taken from the second heating. [f]Decomposition temperature (T_d) determined by TGA at 1% weight loss.

2.2 Spectroscopic analysis

2.2.1 PE-PBD1

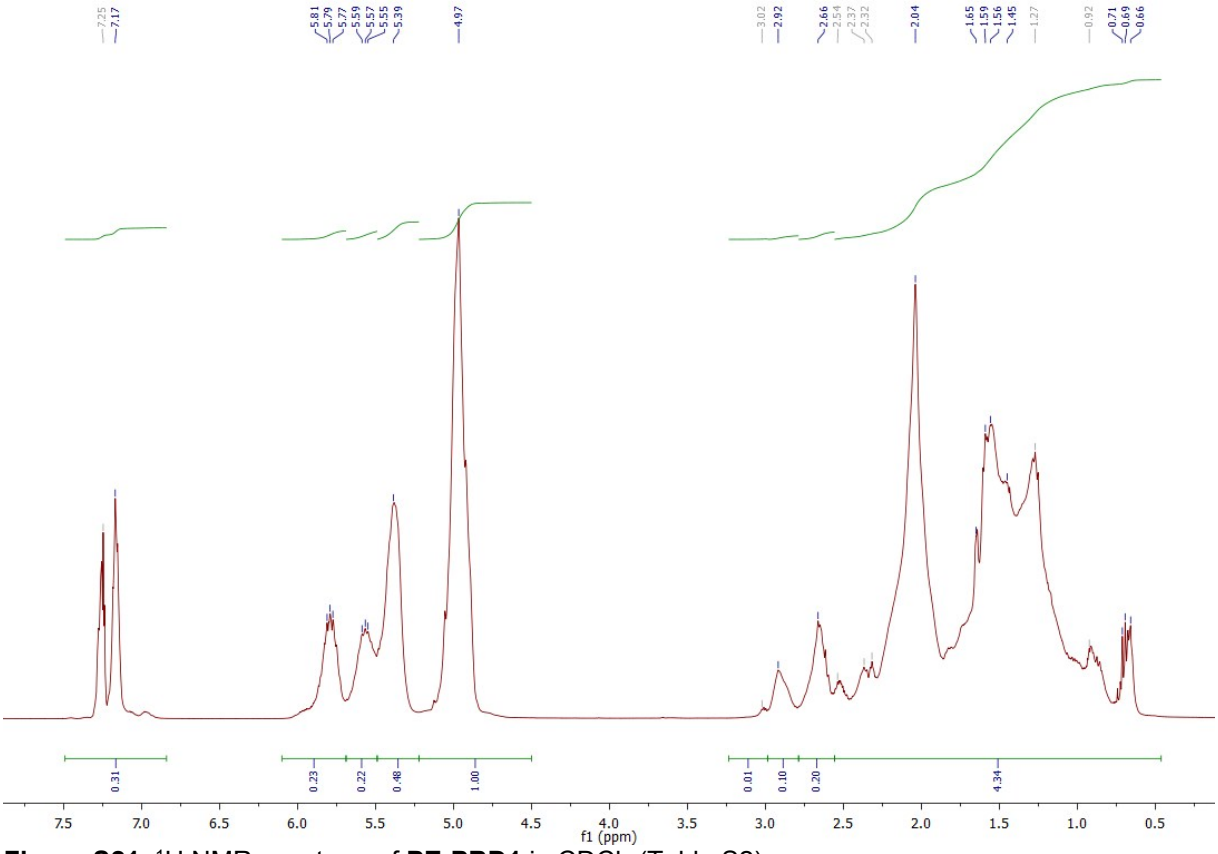

Figure S21. ^{1}H NMR spectrum of **PE-PBD1** in $CDCl_3$ (Table S2).

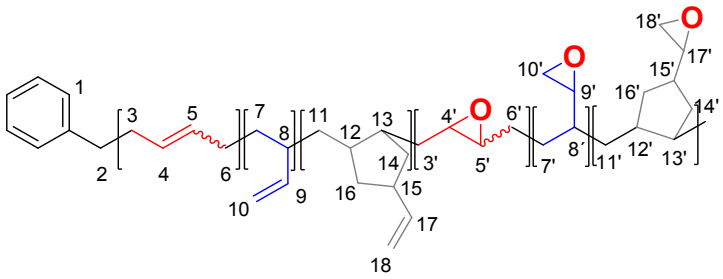

^{1}H NMR ($CDCl_3$, 400 MHz): *δ* (ppm) = 7.50-6.85 (m, 5H, 1-CH),6.0-5.69 (m, 1H, 17-CH), 5.69-5.49 (m, 1H, 9-CH), 5.49-5.22 (m, 2H, 4-CH, 5-CH), 5.23-4.50 (m, 2H, 10-CH_2, 18-CH_2), 3.25-3.00 (m, 2H, 9'-CH, 17'-CH), 3.00-2.80 (m, cis epoxide, 2H, 4'-CH, 5'-CH), 2.80-2.57 (m, trans epoxide, 4H, 2x2-CH, 4'-CH, 5'-CH), 2.57-0.48 (m, 36H, 2x3-CH, 2x3'-CH, 2x6-CH, 2x6'-CH, 2x7-CH, 2x7'-CH, 8-CH, 8'-CH, 2x10'-CH, 2x11-CH, 2x11'-CH, 12-CH, 12'-CH, 13-CH, 13'-CH, 2x14-CH, 2x14'-CH, 15-CH, 15'-CH, 2x16-CH, 2x16'-CH, 2x18'-CH).

Signals from side reactions e. g. epoxide ring opening (-OH formation) and cross-linking (C-O-C formation) typically between *δ* (ppm) = 3 - 6 ppm were not observed for all samples.

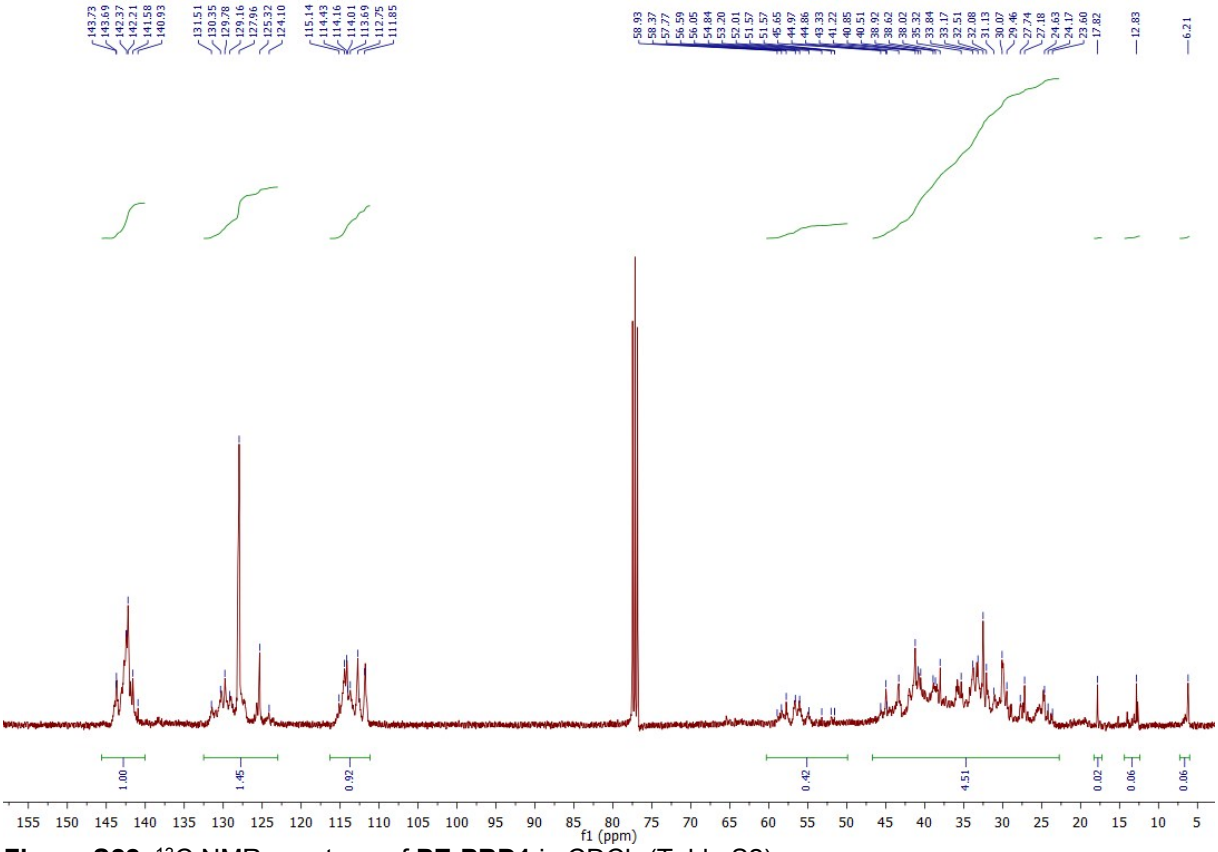

Figure S22. ^{13}C NMR spectrum of **PE-PBD1** in $CDCl_3$ (Table S2).

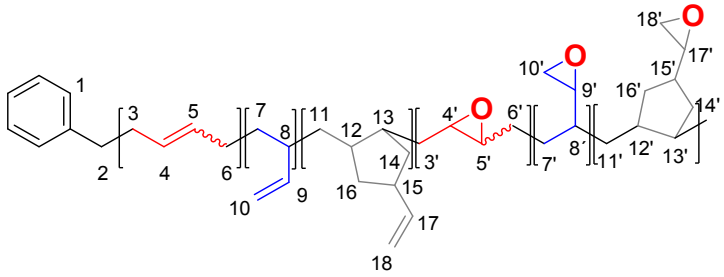

^{13}C NMR ($CDCl_3$, 125 MHz): δ (ppm) = 145.0-141.8 (6x1-C (styrene), 9-C, 17-C), 132.5-123.2 (4-H, 5-C), 115.7-111.5 (10-C, 18-C), 66.0-63.5 (9'-C, 17'-C), 59.5-51.0 (4'-C, 5'-C), 46.7-6.05 (10'-C, 18'-C, 2-C, 3-C, 3'-C, 6-C, 6'-C, 7-C, 7'-C, 8-C, 8'-C, 11-C, 11'-C, 12-C, 12'-C, 13-C, 13'-C, 14-C, 14'-C, 15-C, 15'-C, 16-C, 16'-C).

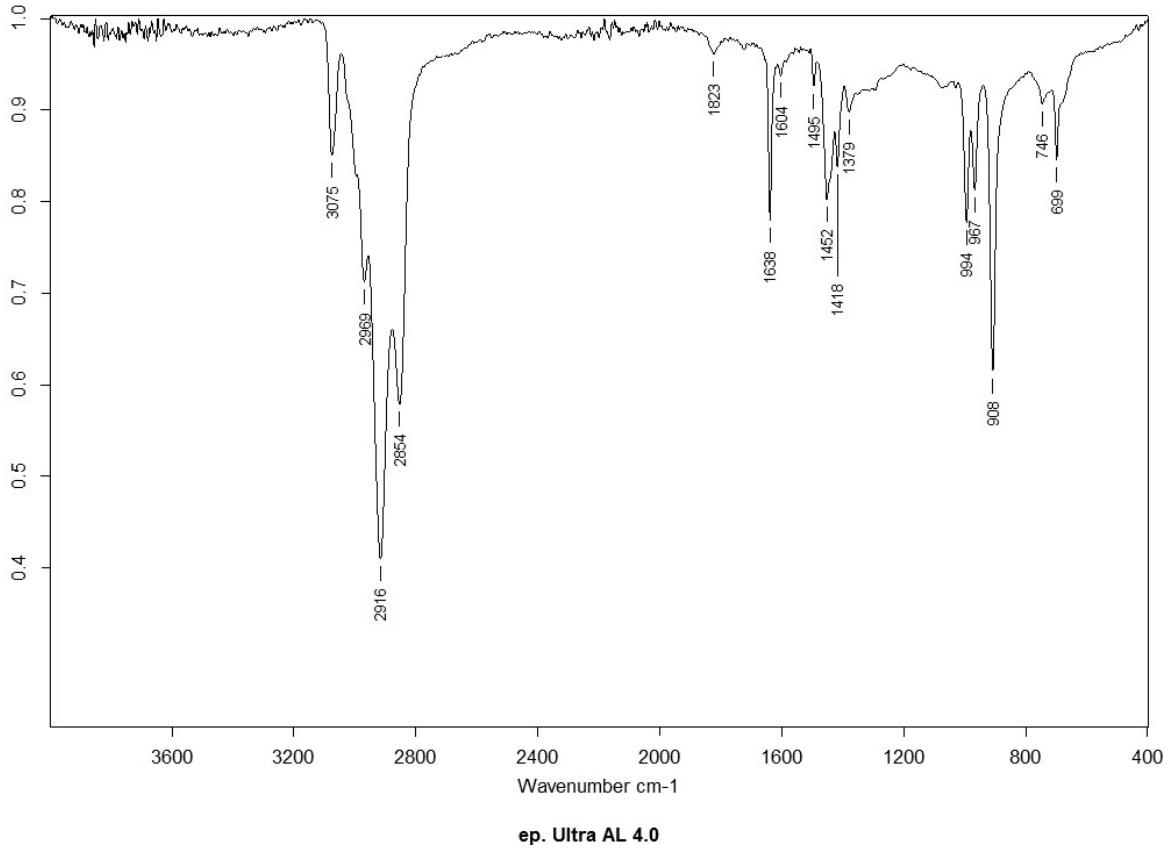

Figure S23. IR spectrum of **PE-PBD1** (Table S2).

Signals from side reactions e. g. epoxide ring opening (-OH formation) and cross-linking (C-O-C formation) typically between 3600 - 3200 cm^{-1} and 1300 - 1000 cm^{-1} were not observed for all samples.

2.2.2 PE-PBD2

Please note the peak assignments in Figure S21 and S22. The signal for 1, 4-cis and 1, 4-trans double bonds splits into the signals at δ (ppm) = 5.45 (m, 2H (trans)) and 5.42 (m, 2H, (cis)).

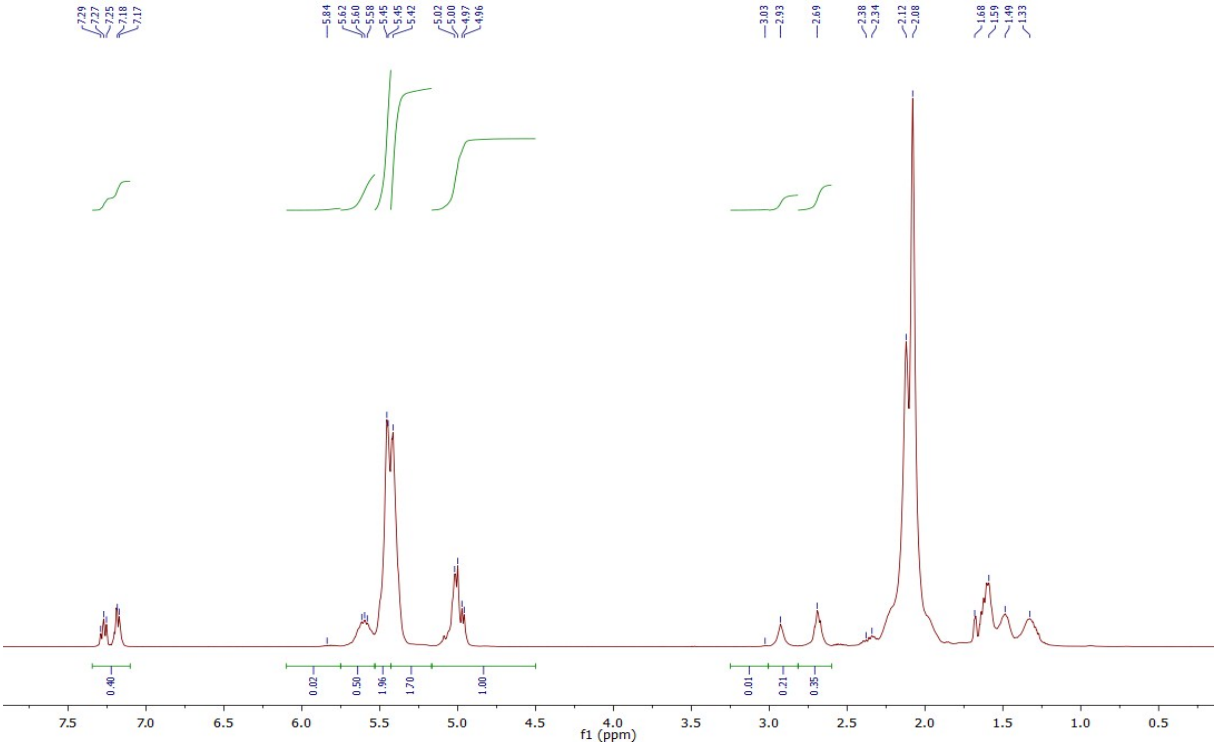

Figure S24. ^{1}H NMR spectrum of **PE-PBD2** in $CDCl_3$ (Table S2).

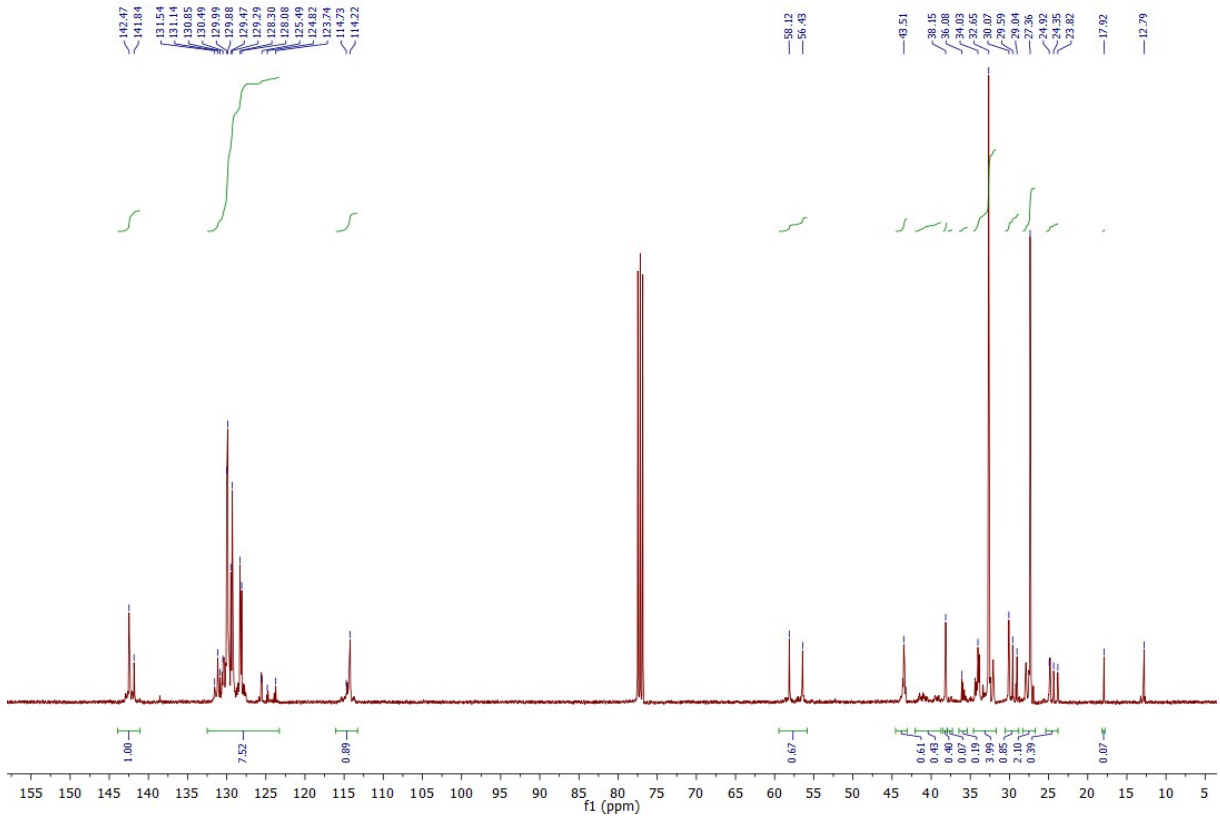

Figure S25. ^{13}C NMR spectrum of **PE-PBD2** in $CDCl_3$ (Table S2).

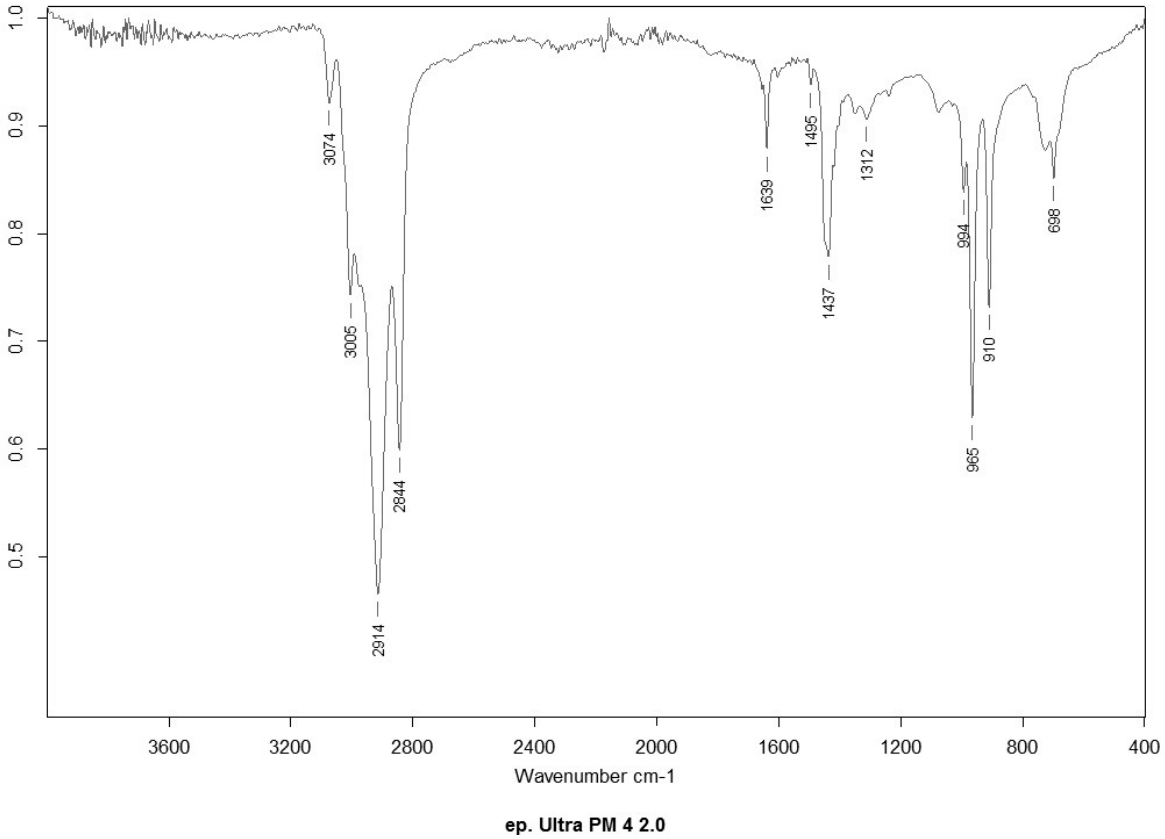

Figure S26. IR spectrum of **PE-PBD2** (Table S2).

2.2.3 PE-PBD3

Please note the peak assignments in Figure S21 and S22.The signal for 1, 4-cis and 1, 4-trans double bonds splits into the signals at δ (ppm) = 5.36 (m, 2H (trans)) and 5.32 (m, 2H, (cis)).

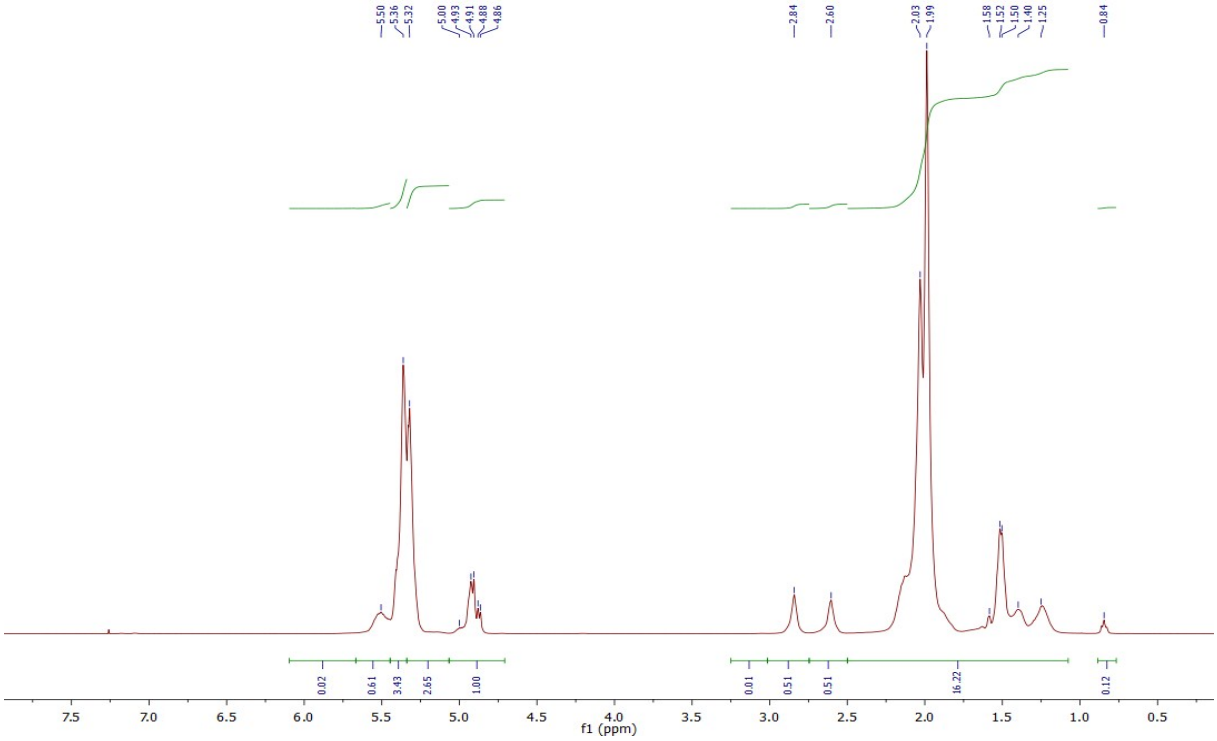

Figure S27. ^{1}H NMR spectrum of **PE-PBD3** in $CDCl_3$ (Table S2).

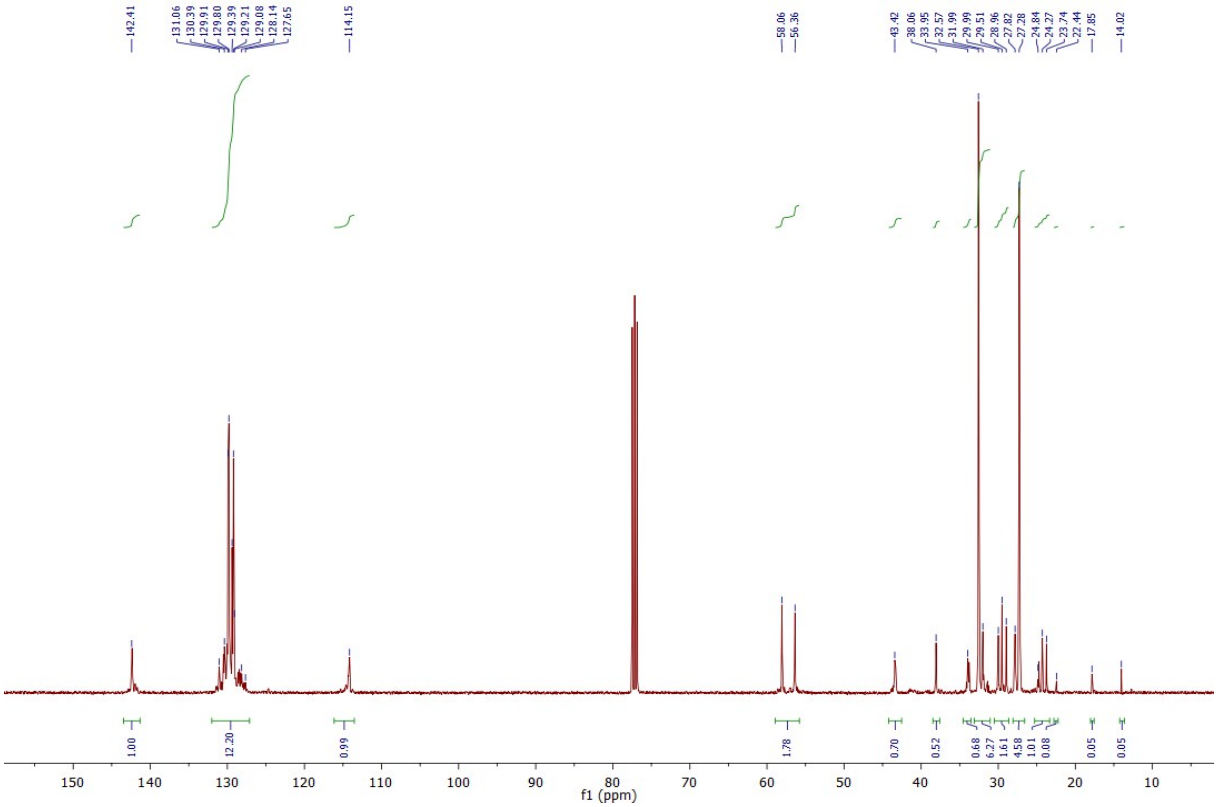

Figure S28. ^{13}C NMR spectrum of **PE-PBD3** in $CDCl_3$ (Table S2).

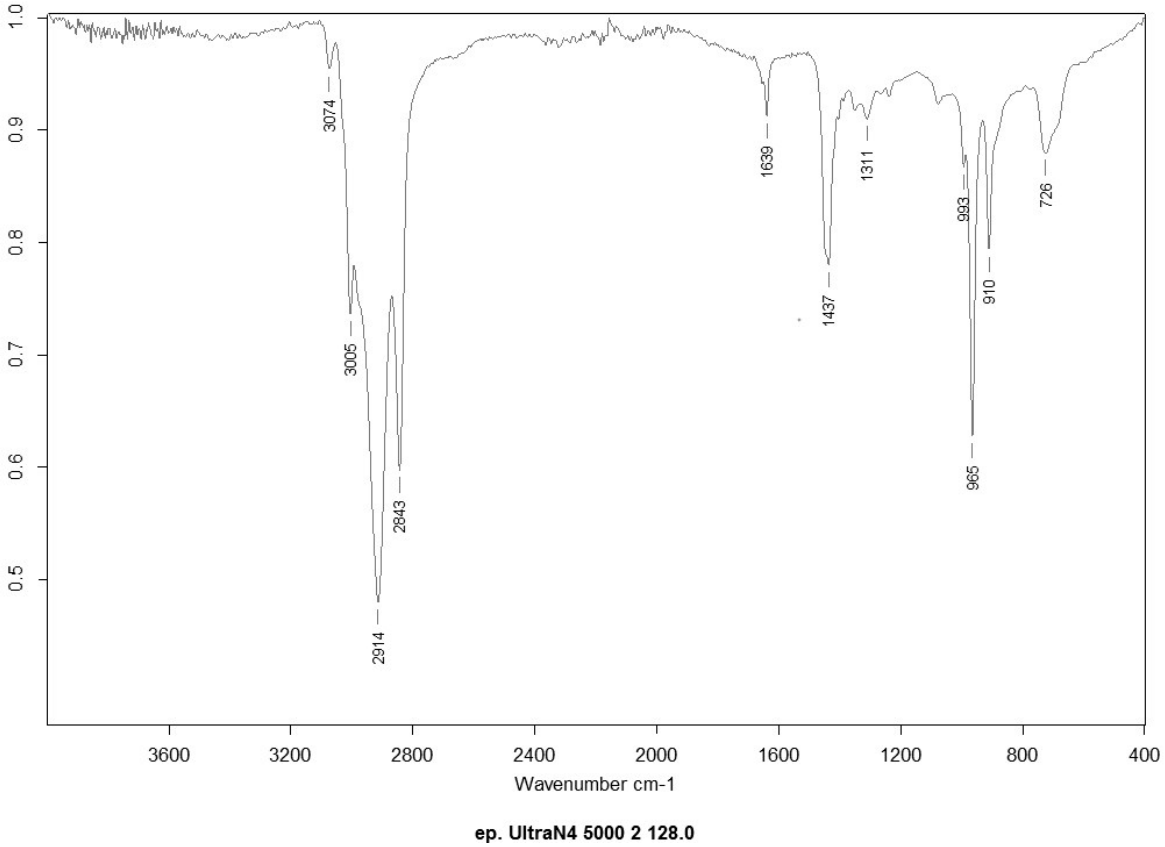

Figure S29. IR spectrum of **PE-PBD3** (Table S2).

2.2.4 PE-PBD4

Please note the peak assignments in Figure S21 and S22.The signal for 1, 4-cis and 1, 4-trans double bonds splits into the signals at δ (ppm) = 5.40 (m, 2H (trans)) and 5.36 (m, 2H, (cis)).

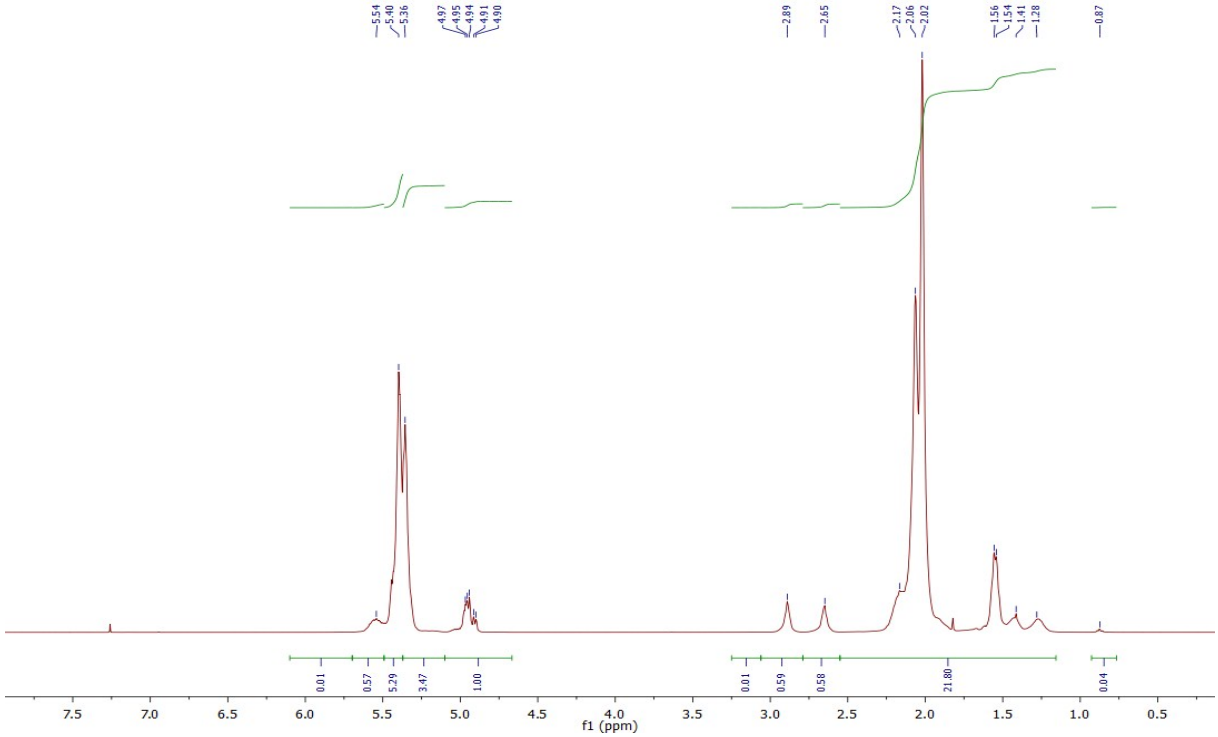

Figure S30. ^{1}H NMR spectrum of **PE-PBD4** in $CDCl_3$ (Table S2).

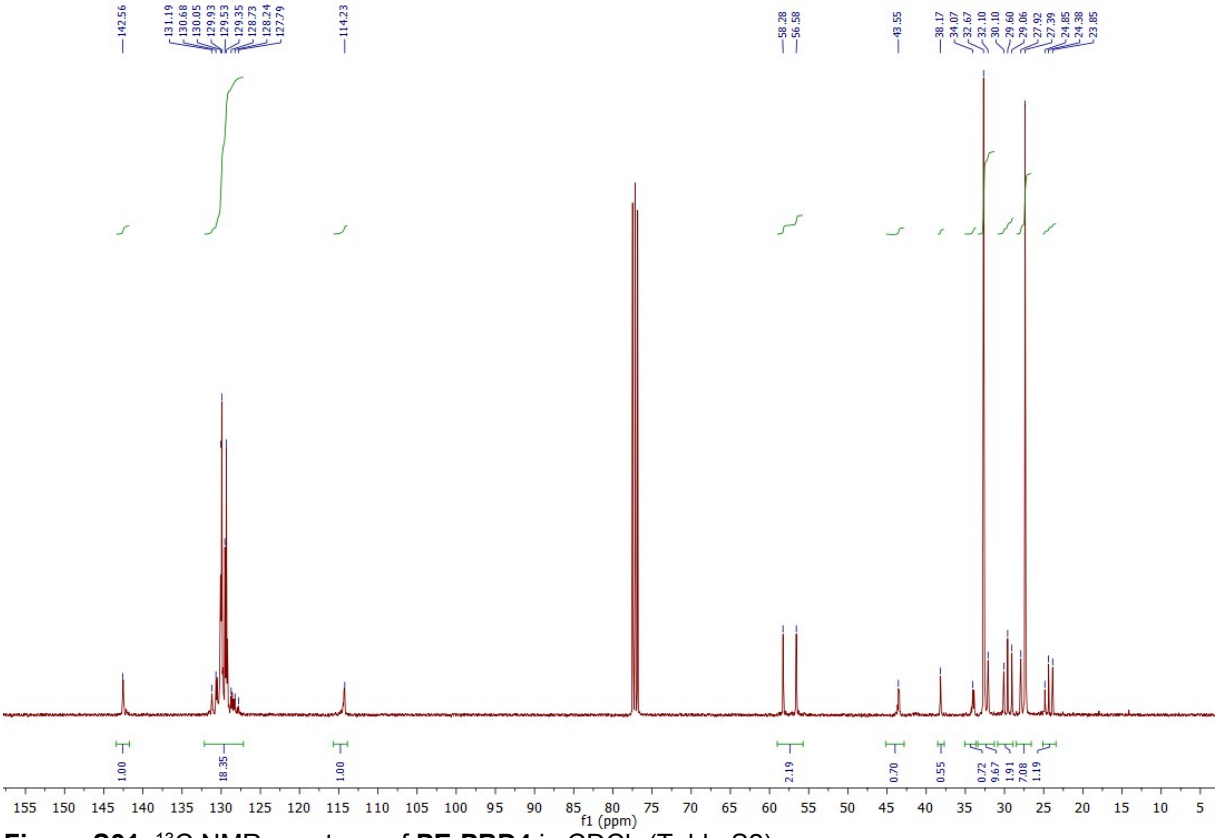

Figure S31. ^{13}C NMR spectrum of **PE-PBD4** in $CDCl_3$ (Table S2).

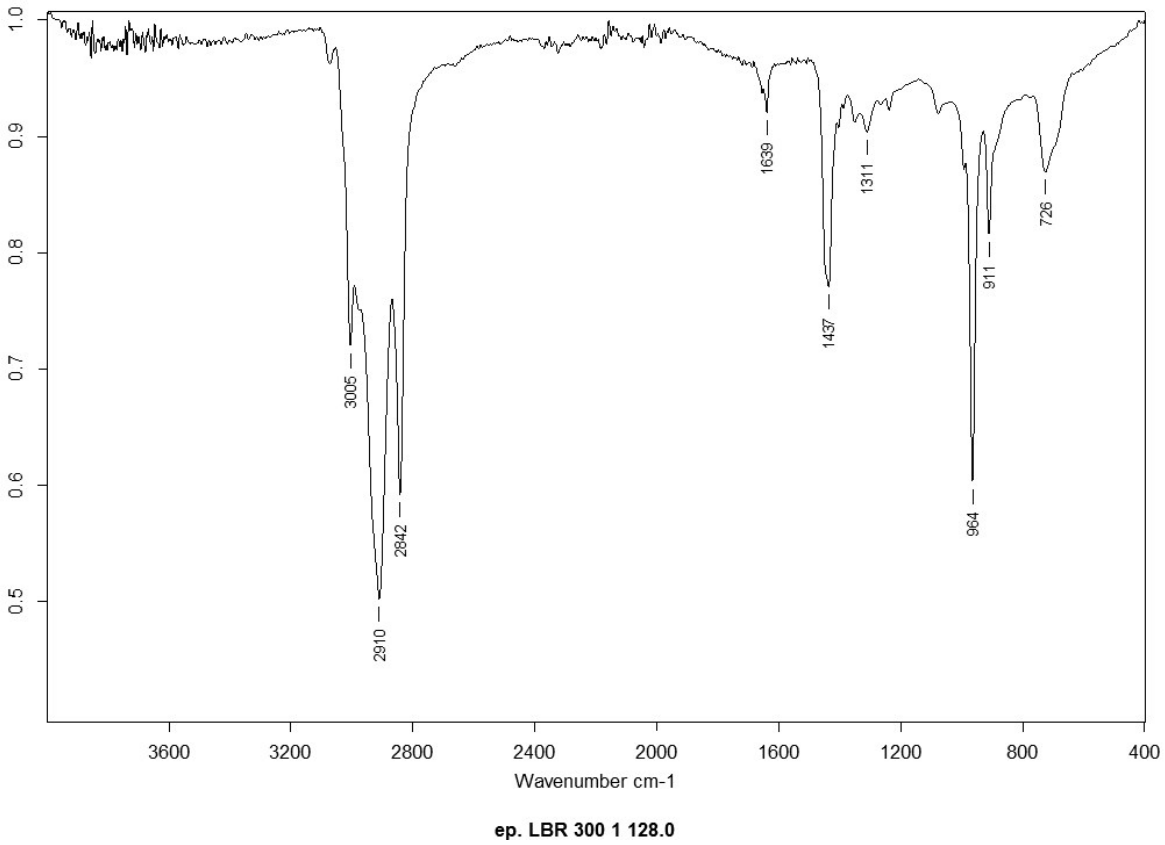

Figure S32. IR spectrum of **PE-PBD4** (Table S2).

2.3Thermal analysis

2.3.1 PE-PBD1

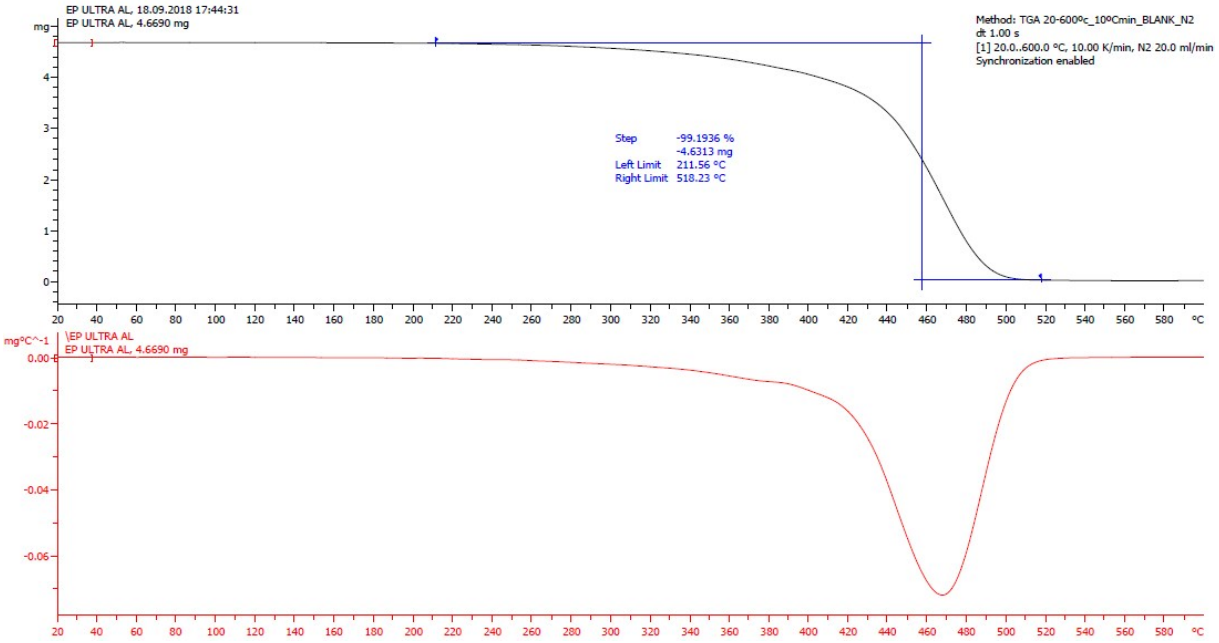

Figure S33. Thermogravimetric analysis of **PE-PBD1** (Table S2).

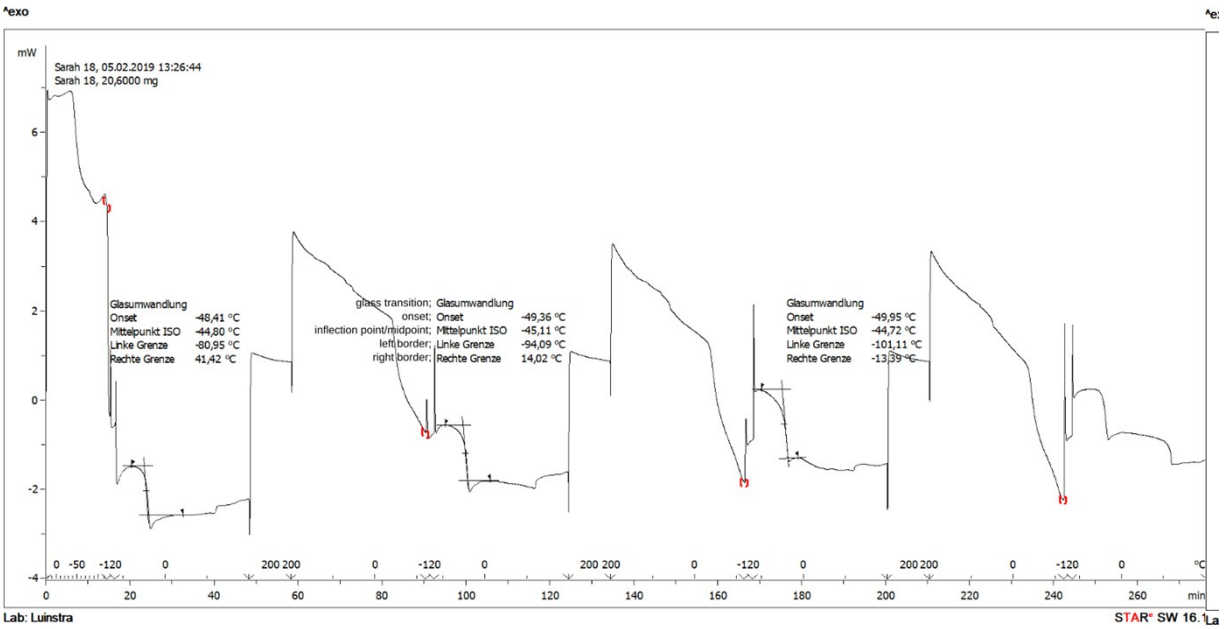

Figure S34. Differential Scanning Calorimetry trace of **PE-PBD1** (Table S2).

2.3.2 PE-PBD2

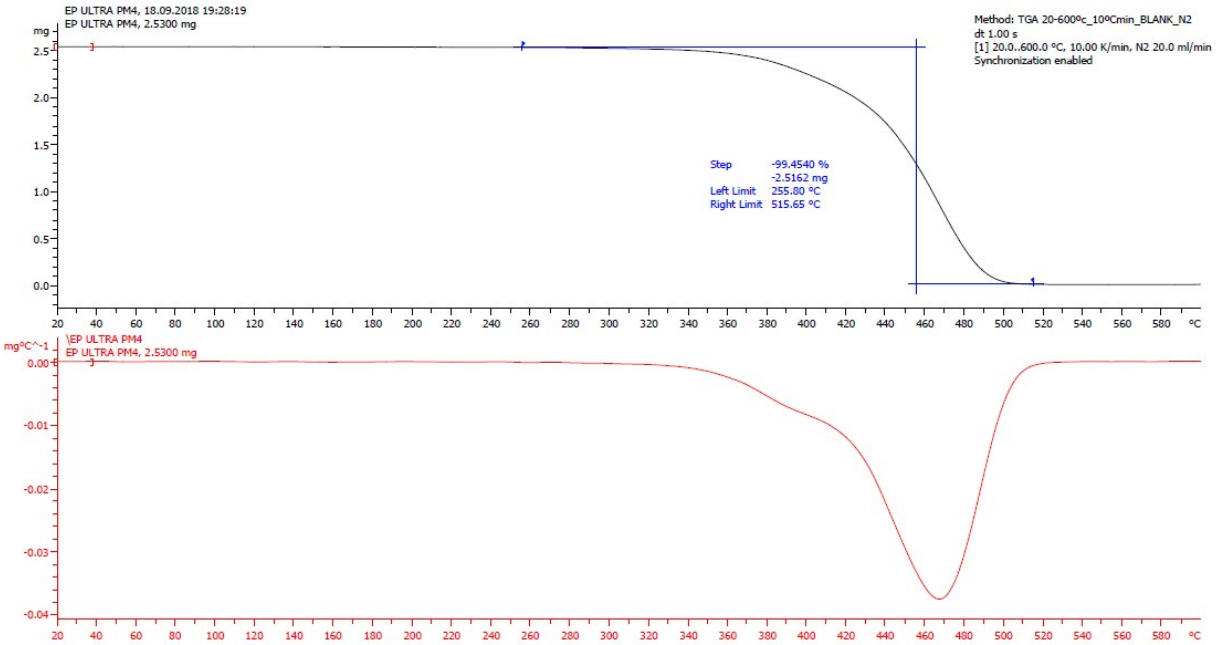

Figure S35. Thermogravimetric analysis of **PE-PBD2** (Table S2).

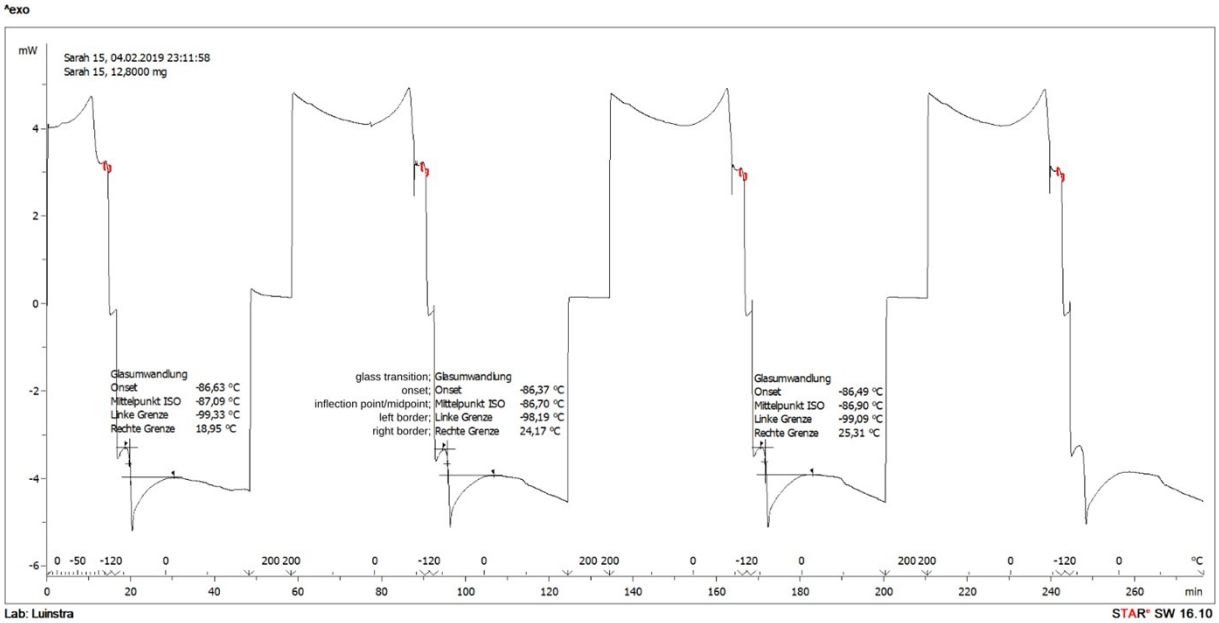

Figure S36. Differential Scanning Calorimetry trace of **PE-PBD2** (Table S2).

2.3.3 PE-PBD3

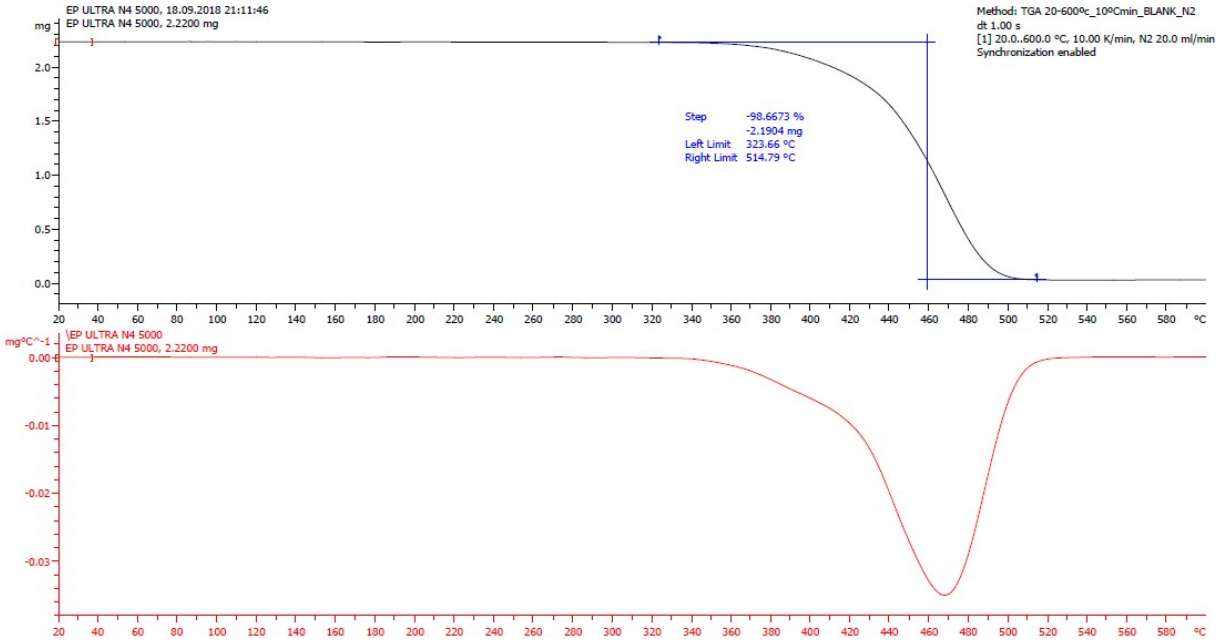

Figure S37. Thermogravimetric analysis of **PE-PBD3** (Table S2).

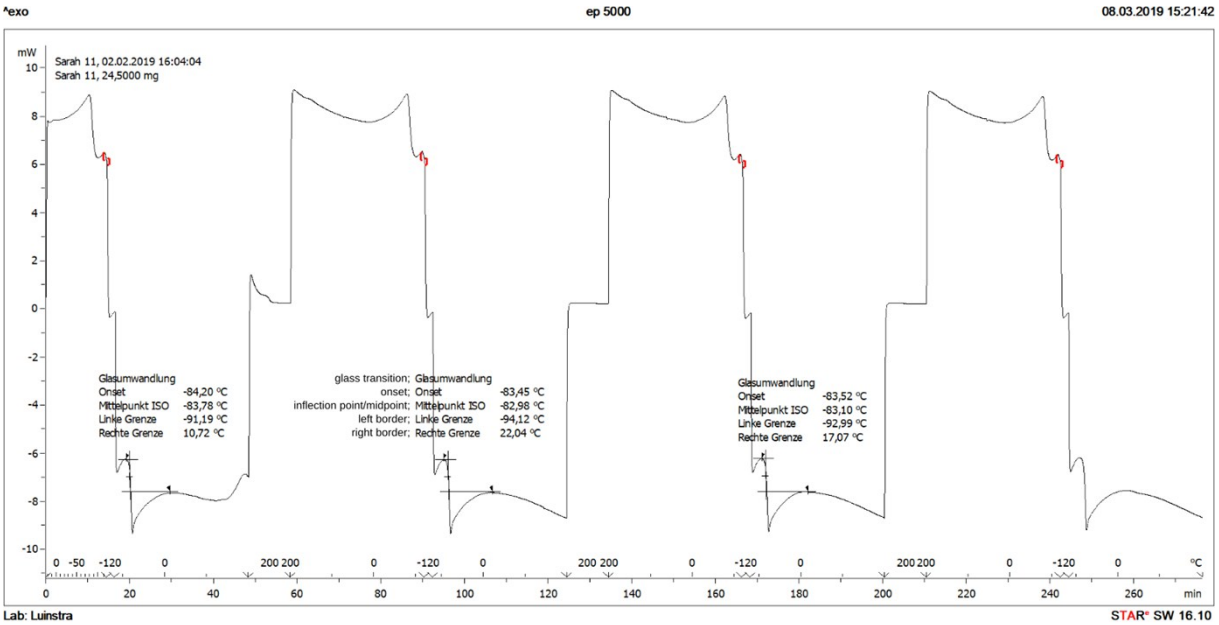

Figure S38. Differential Scanning Calorimetry trace of **PE-PBD3** (Table S2).

2.3.4 PE-PBD4

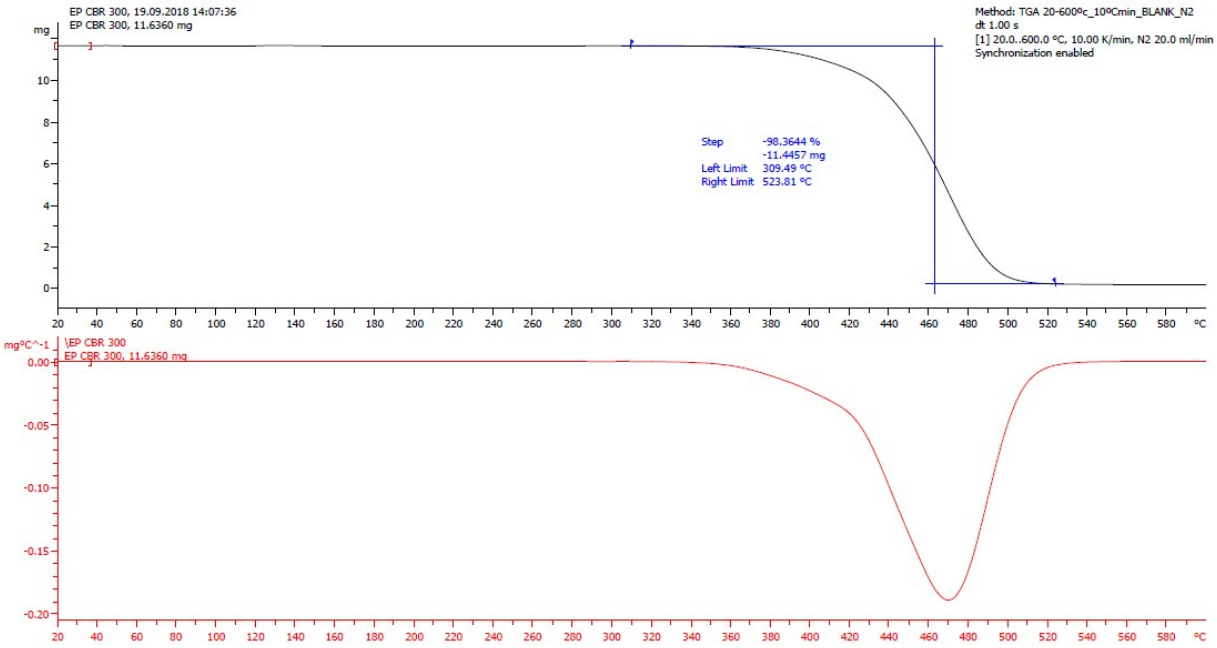

Figure S39. Thermogravimetric analysis of **PE-PBD4** (Table S2).

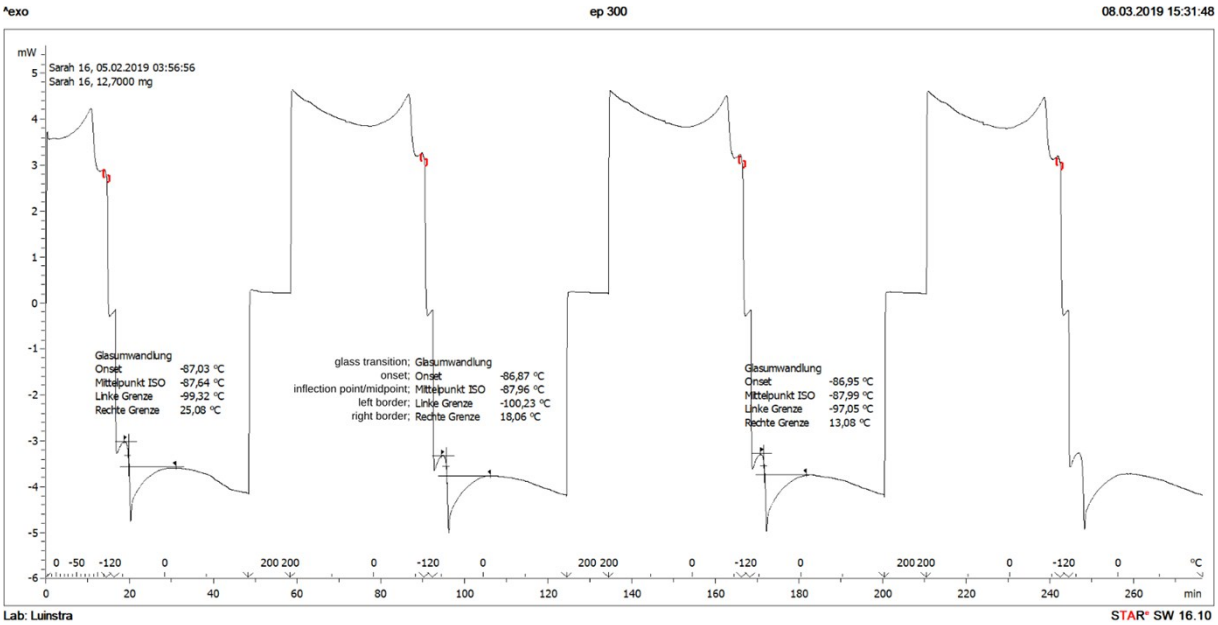

Figure S40. Differential Scanning Calorimetry trace of **PE-PBD4** (Table S2).

3. Determination of PBDs double bond contents

EP-numbers of several partly epoxidized PBDs were determined by the titration technique described in the Experimental Section. The relative amounts of converted double bonds were calculated by ^{1}H NMR analysis. Both results were applied to the graph shown in figure S41.

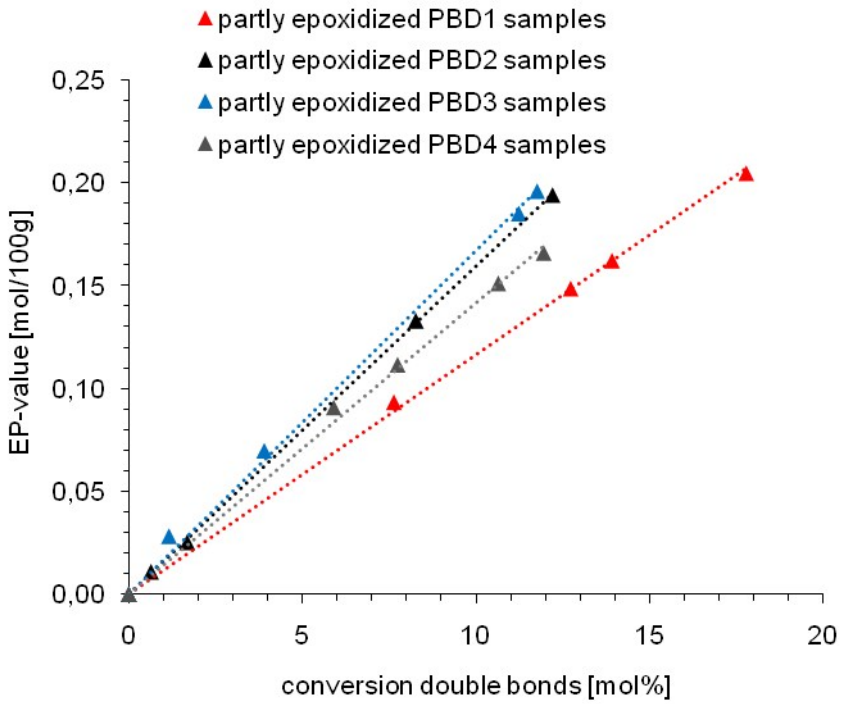

Figure S41. EP-numbers of partly epoxidized PBDs and relative amount of epoxidized double bonds applied to a graph and linearly fitted.

Linear fitting and extrapolation leads to the EP-values expectable at 100 % epoxide conversion. This is equated with the total amount of double bonds in the polymers, respectively. The results are summarized in table S3. All samples differ from the theoretical value of 18.5 mmol/g.

Table S3. Summary of data derived by linear fit and extrapolation.

PBD	slope, a $[\frac{[mol/100g}{mol\%}]$	coefficient of determination, R^2	EP-value at 100% epoxide conversion [mol/100g]
PBD1	0.0117	0.9990	1.17
PBD2	0.0160	0.9998	1.60
PBD3	0.0167	0.9967	1.67
PBD4	0.0142	0.9962	1.42

4. Characterization of PC-PBDs

4.1 Spectroscopic analysis

4.1.1 PC-PBD1

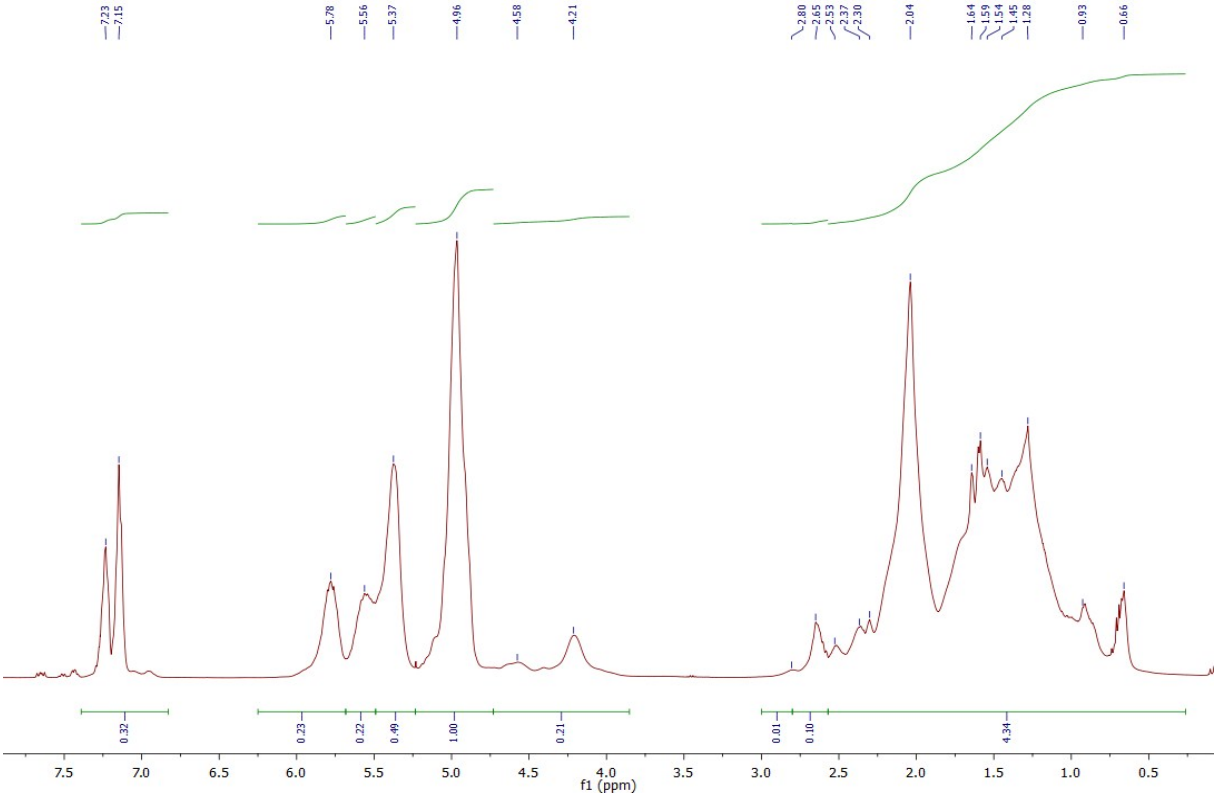

Figure S42. ^{1}H NMR spectrum of **PC-PBD1** in $CDCl_3$ (Table 2).

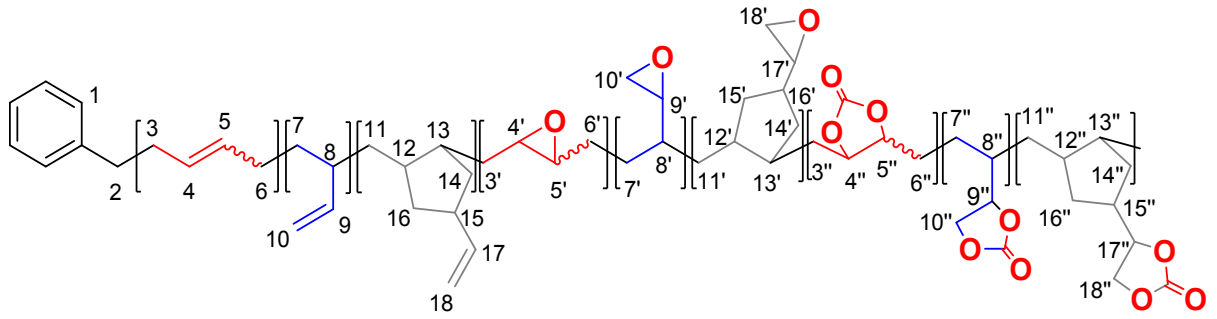

^{1}H NMR ($CDCl_3$, 400 MHz): δ (ppm) = 7.39-6.85 (m, 5H, 1-CH),6.25-5.68(m, 1H, 17-CH), 5.68-5.49 (m, 1H, 9-CH), 5.49-5.23 (m, 2H, 4-CH, 5-CH), 5.23-4.73 (m, 2H, 10-CH_2, 18-CH_2), 4.73-3.85 (m, 8H, 4''-H, 5''-H, 9''-H, 10''-H, 17''-H, 18''-H), 3.25-3.00 (m, 2H, 9'-CH, 17'-CH), 3.00-2.80 (m, cis-epoxide, 2H, 4'-CH, 5'-CH), 2.80-2.57 (m, trans-epoxide, 4H, 2x2-CH, 4'-CH, 5'-CH), 2.57-0.48 (m, 52H, 2x3-CH, 2x3'-CH, 2x3''-CH, 2x6-CH, 2x6'-CH, 2x6''-CH, 2x7-CH, 2x7'-CH, 2x7''-CH 8-CH, 8'-CH, 8''-CH, 2x10'-CH, 2x11-CH, 2x11'-CH, 2x11''-CH 12-CH, 12'-CH, 12''-CH, 13-CH, 13'-CH,13''-CH, 2x14-CH, 2x14'-CH, 2x14''-CH, 15-CH, 15'-CH, 15''-CH, 2x16-CH, 2x16'-CH, 2x16''-CH).

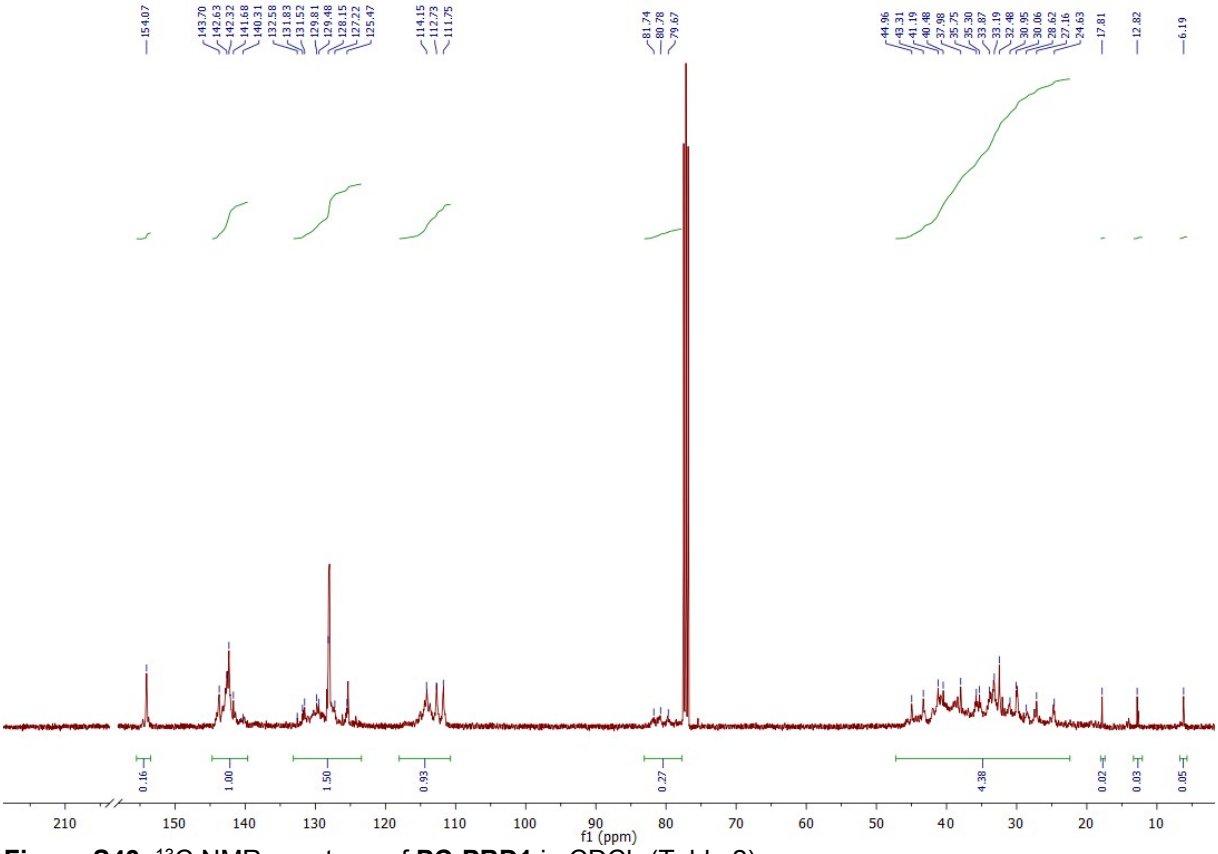

Figure S43. ^{13}C NMR spectrum of **PC-PBD1** in $CDCl_3$ (Table 2).

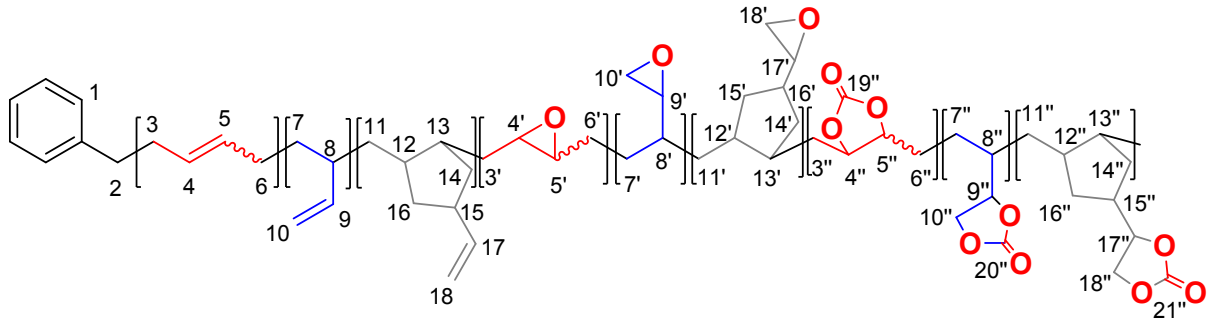

^{13}C NMR ($CDCl_3$, 125 MHz): δ (ppm) = 145.0-141.8 (6x1-C (styrene), 9-C, 17-C), 132.5-123.2 (4-H, 5-C), 115.7-111.5 (10-C, 18-C), 83.0-77.7 (4''-C, 5''-C, 9''-C, 10''-C, 17''-C, 18''-C), 66.0-63.5 (9'-C, 17'-C), 59.5-51.0 (4'-C, 5'-C), 46.7-6.05 (2-C, 3-C, 3'-C, 3''-C, 6-C, 6'-C, 6''-C, 7-C, 7'-C, 7''-C, 8-C, 8'-C, 8''-C,11-C, 11'-C, 11''-C, 12-C, 12'-C, 12''-C, 13-C, 13'-C, 13''-C, 14-C, 14'-C, 14''-C, 15-C, 15'-C, 15''-C, 16-C, 16'-C, 16''-C).

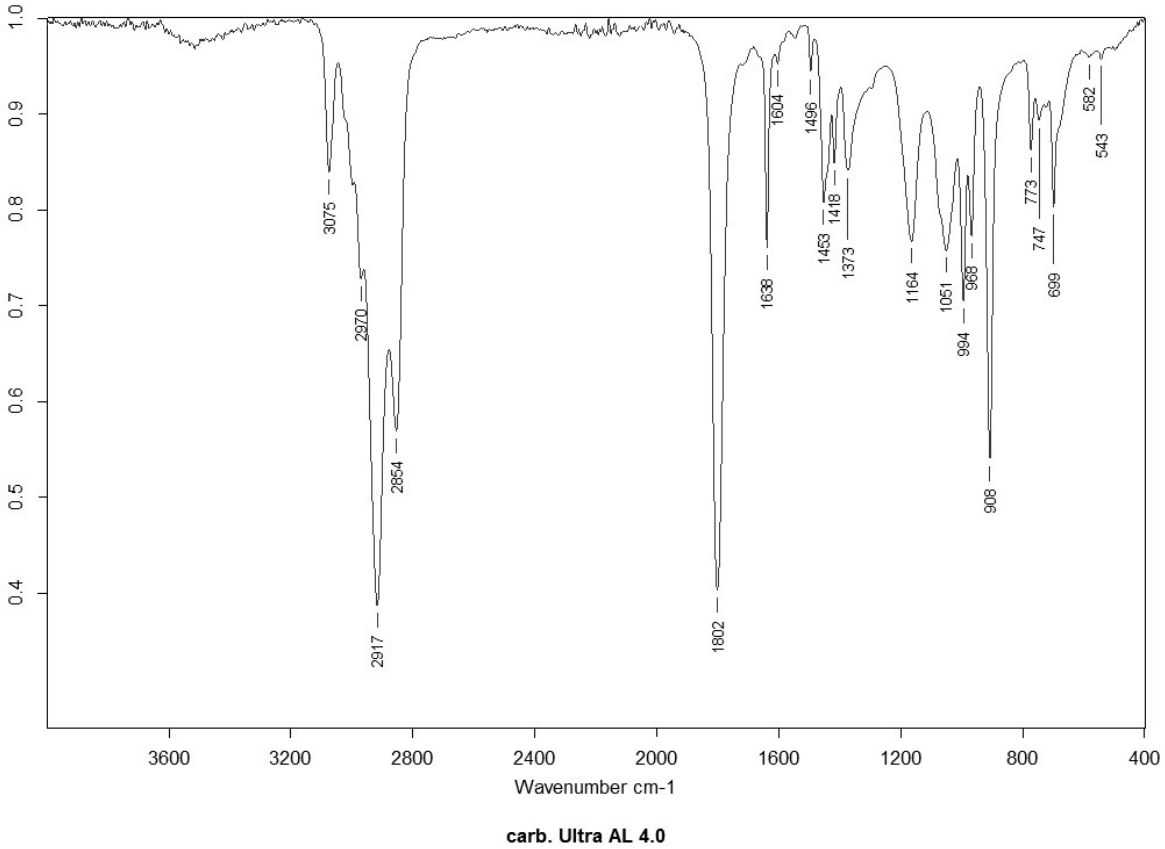

Figure S44. IR spectrum of **PC-PBD1** (Table 2).

4.1.2 PC-PBD2

Please note the peak assignments in Figure S42 and S43.

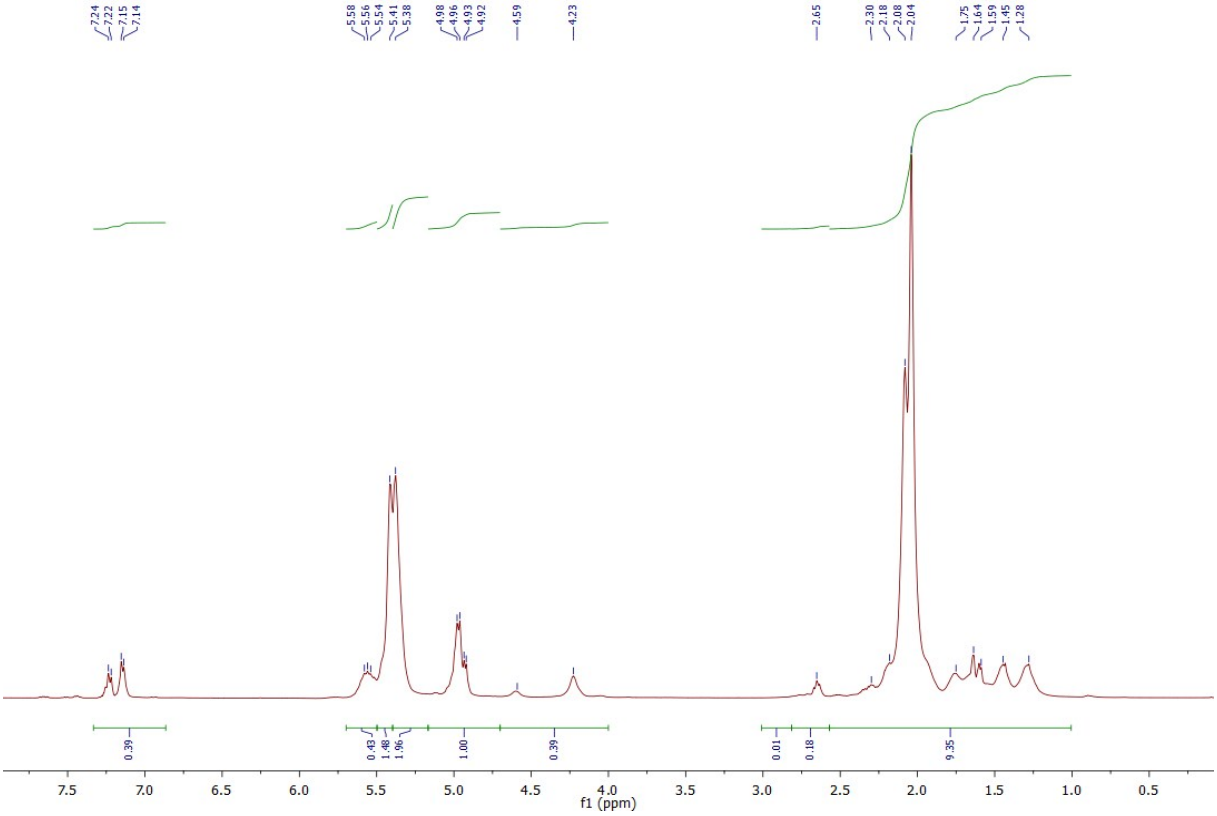

Figure S45. ^{1}H NMR spectrum of **PC-PBD2** in $CDCl_3$ (Table 2).

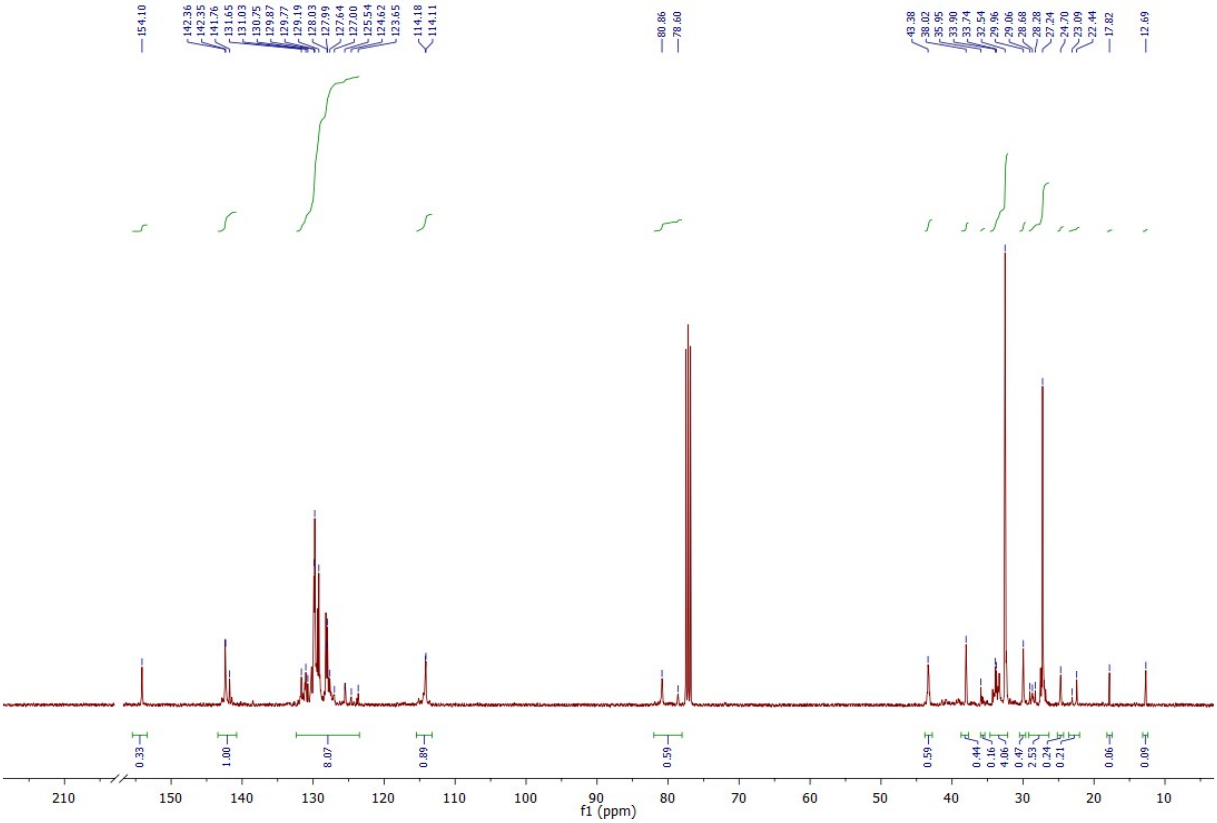

Figure S46. ^{13}C NMR spectrum of **PC-PBD2** in $CDCl_3$ (Table 2).

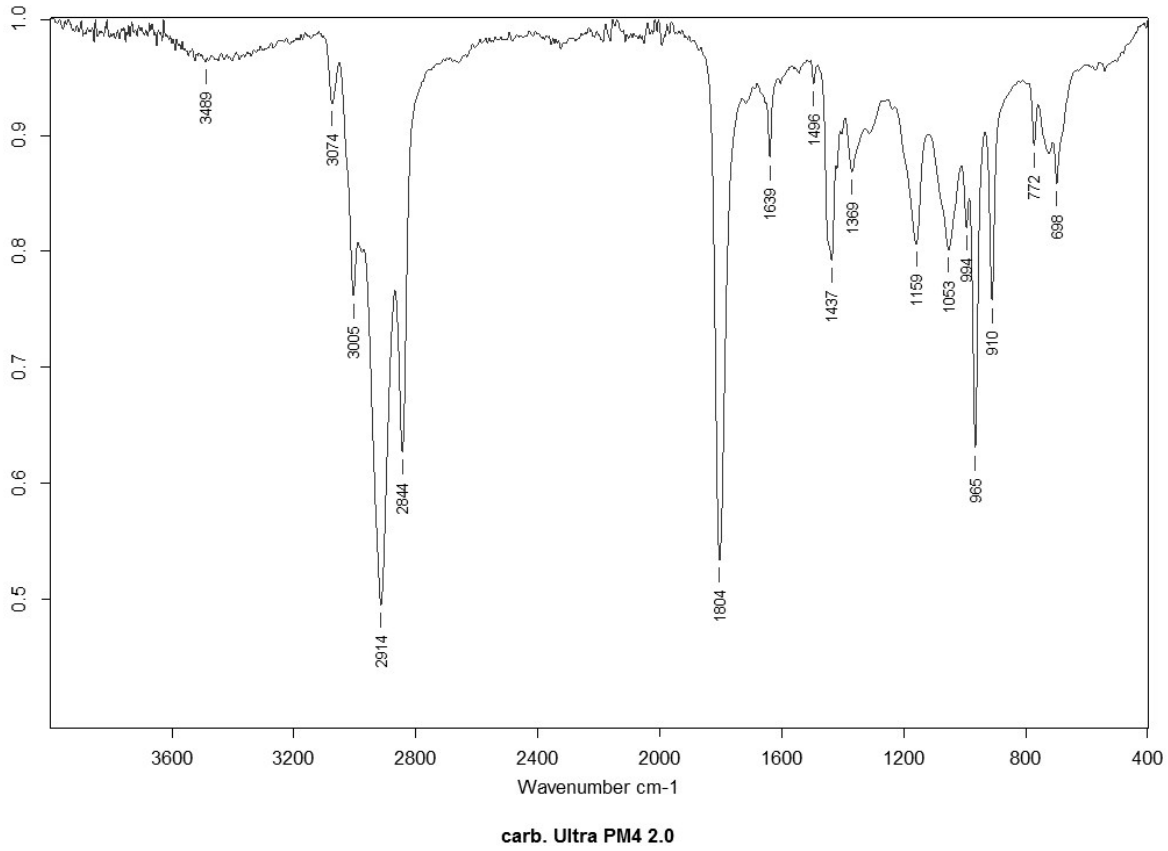

Figure S47. IR spectrum of **PC-PBD2** (Table 2).

4.1.3 PC-PBD3

Please note the peak assignments in Figure S42 and S43.

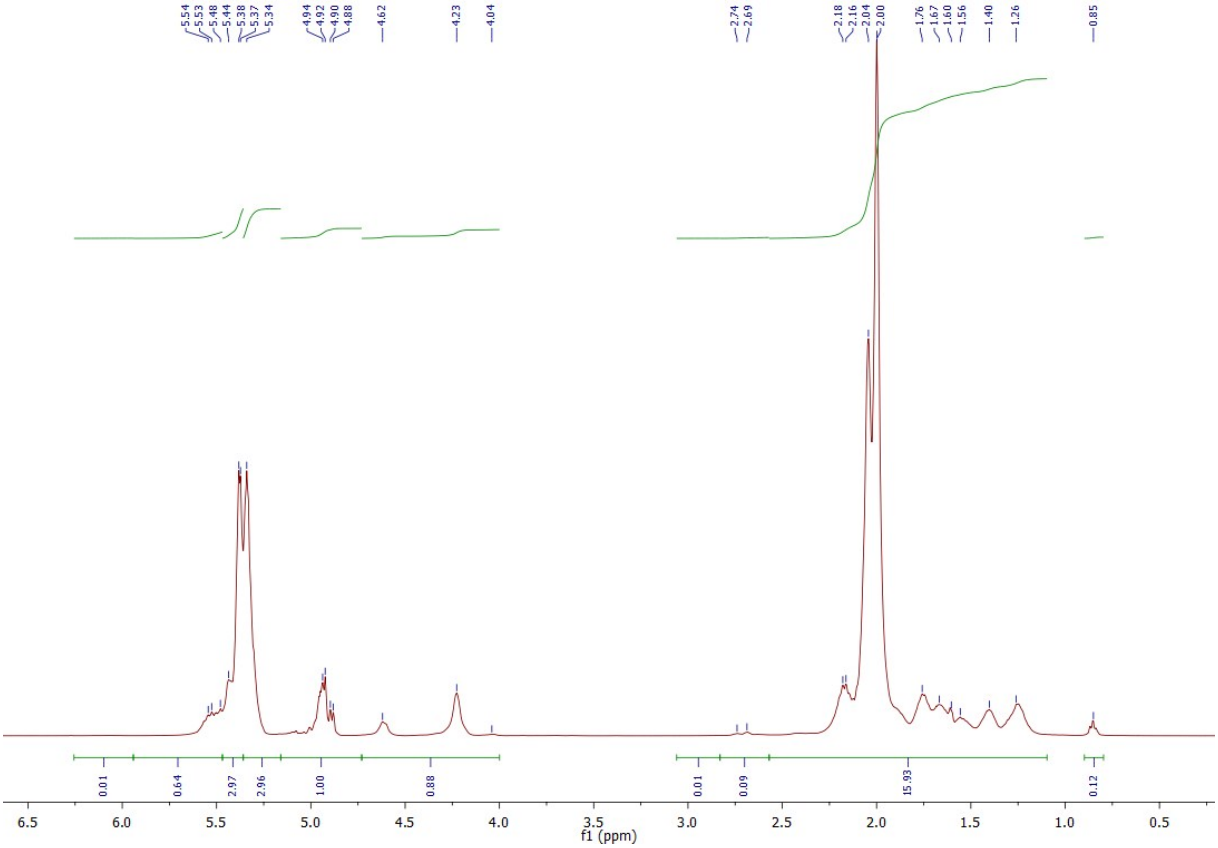

Figure S48. ^{1}H NMR spectrum of **PC-PBD3** in $CDCl_3$ (Table 2).

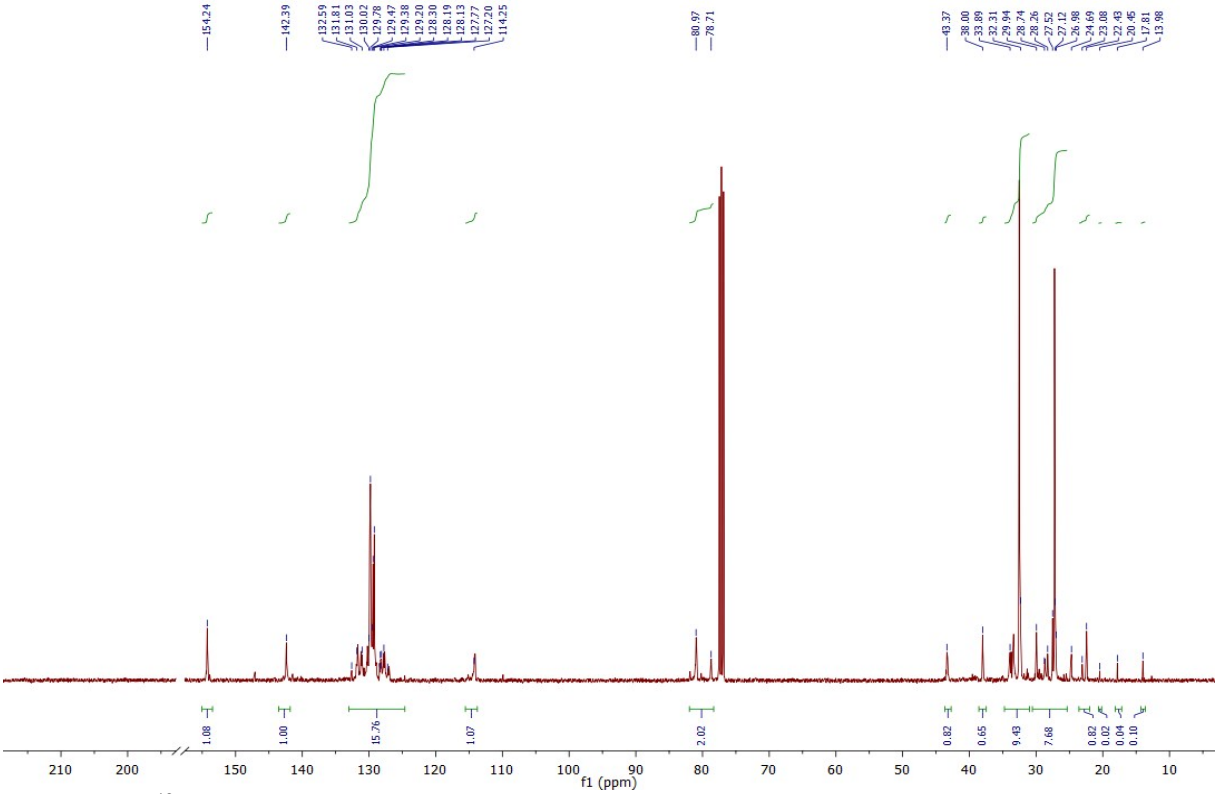

Figure S49. ^{13}C NMR spectrum of **PC-PBD3** in $CDCl_3$ (Table 2).

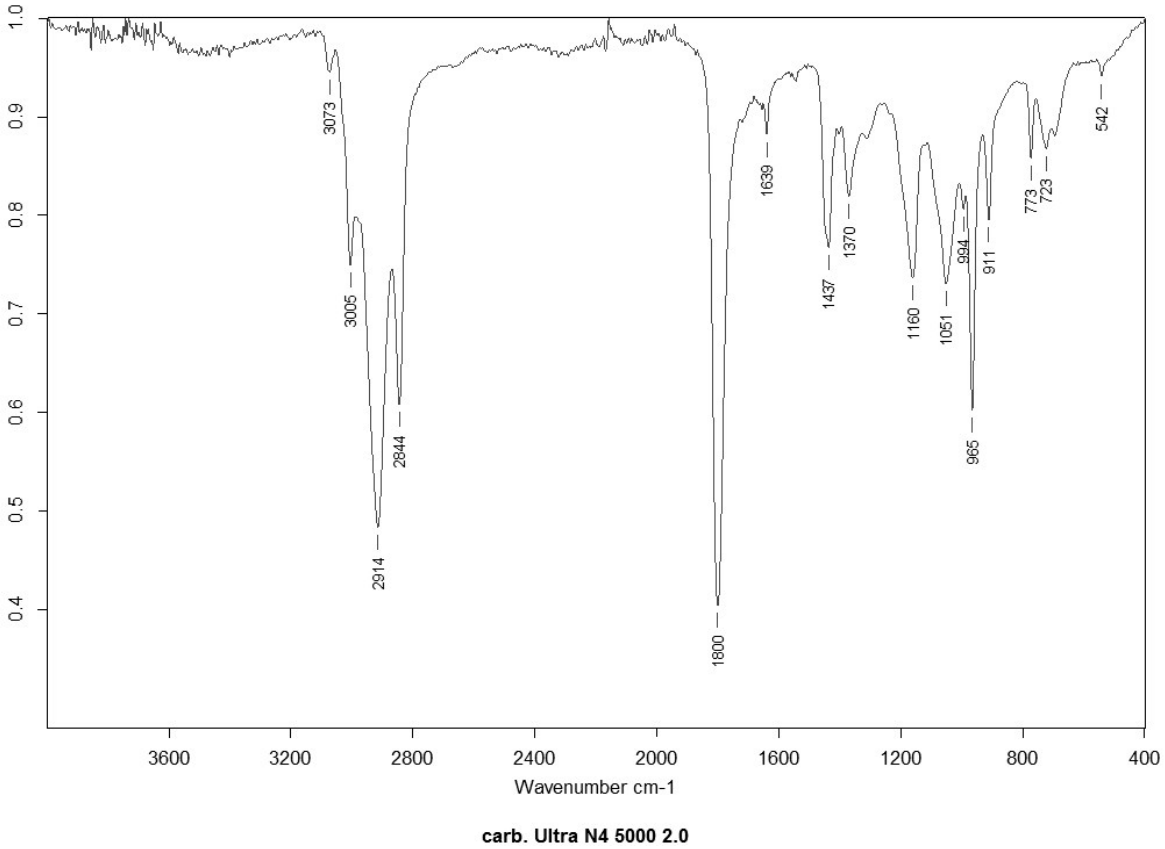

Figure S50. IR spectrum of **PC-PBD3** (Table 2).

4.1.4 PC-PBD4

Please note the peak assignments in Figure S42 and S43.

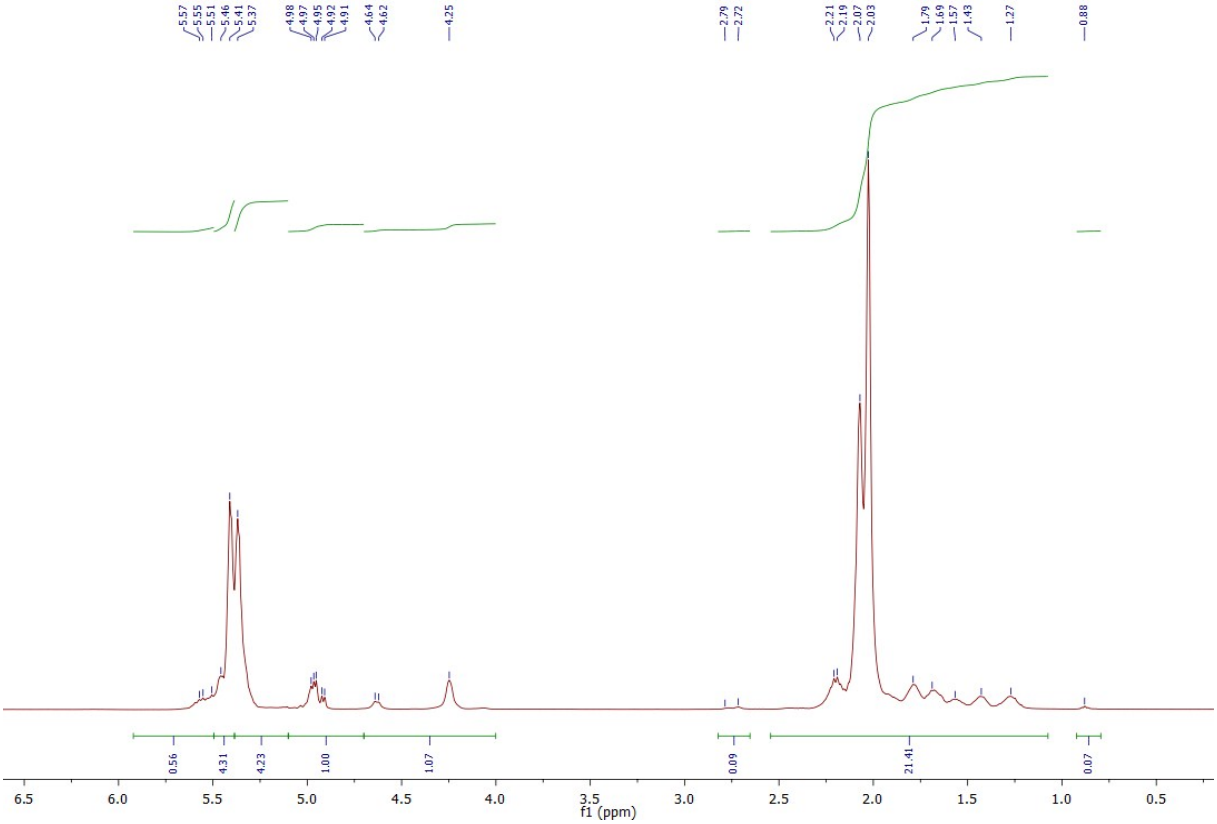

Figure S51. ^{1}H NMR spectrum of **PC-PBD4** in $CDCl_3$ (Table 2).

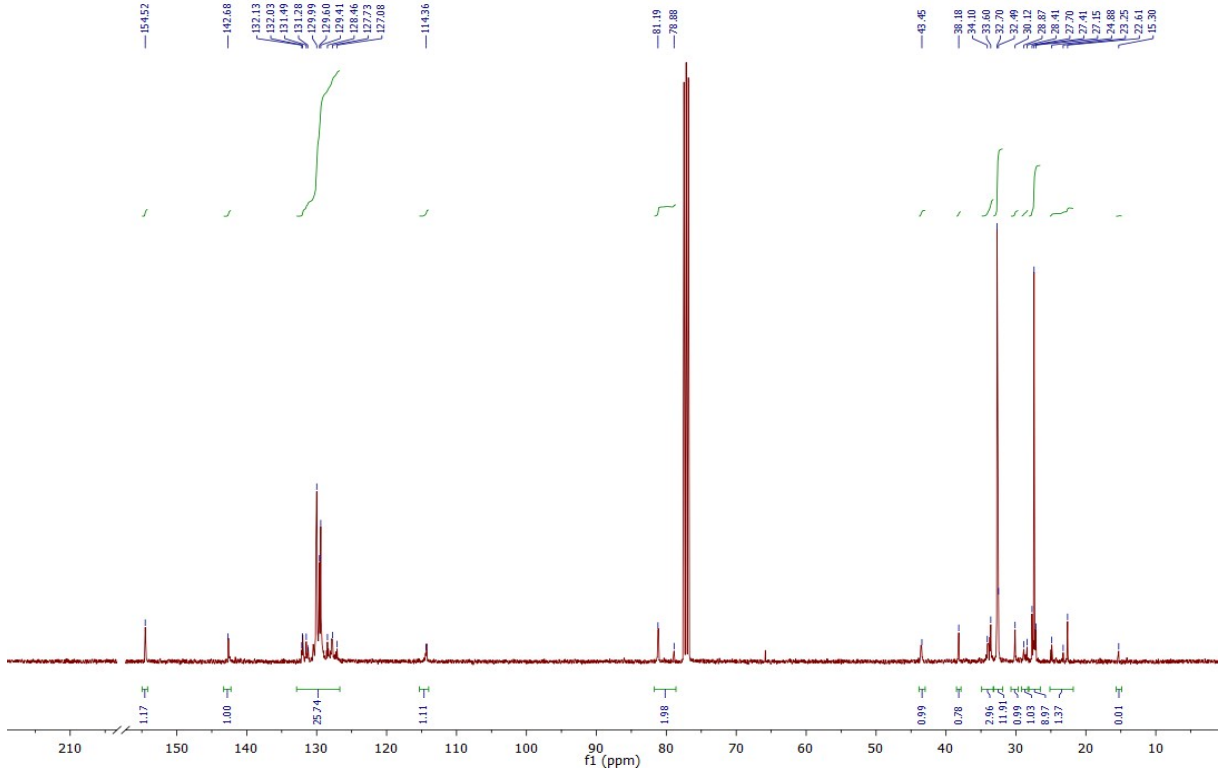

Figure S52. ^{13}C NMR spectrum of **PC-PBD4** in $CDCl_3$ (Table 2).

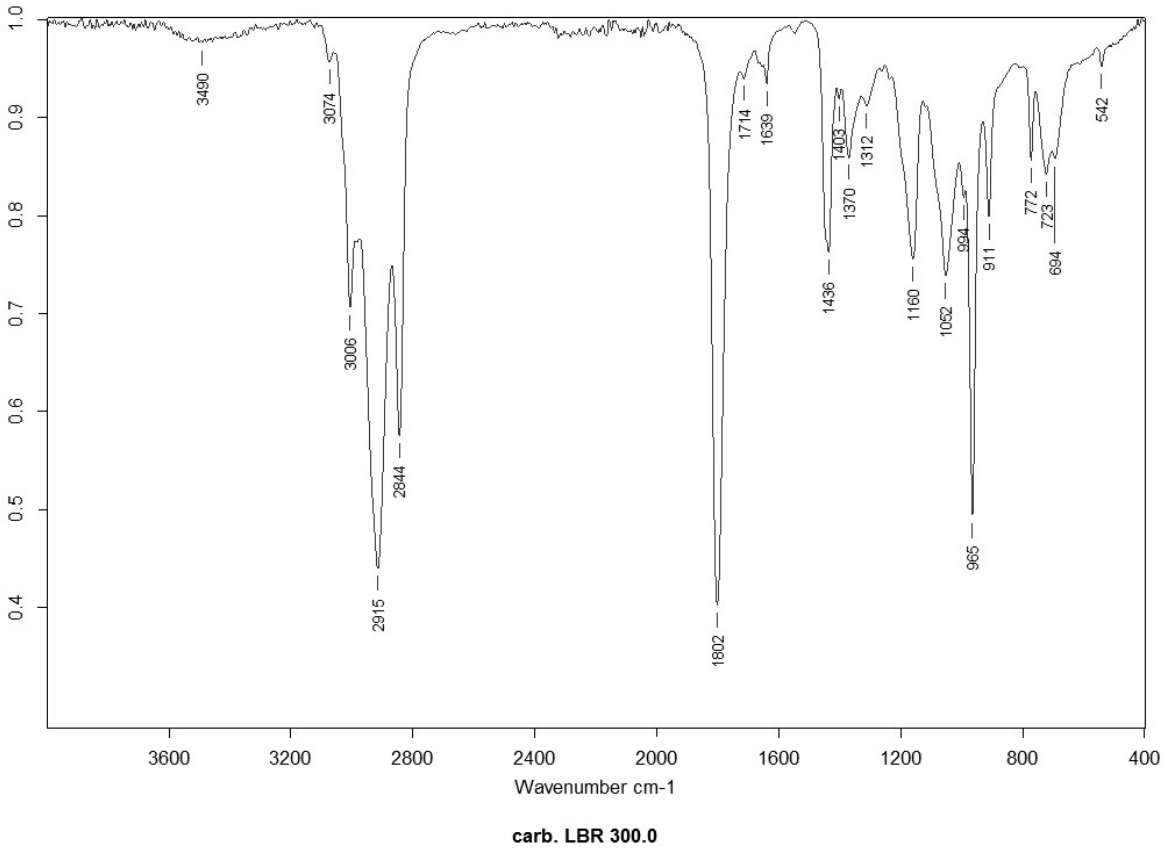

Figure S53. IR spectrum of **PC-PBD4** (Table 2).

4.2 Thermal analysis

4.2.1 PC-PBD1

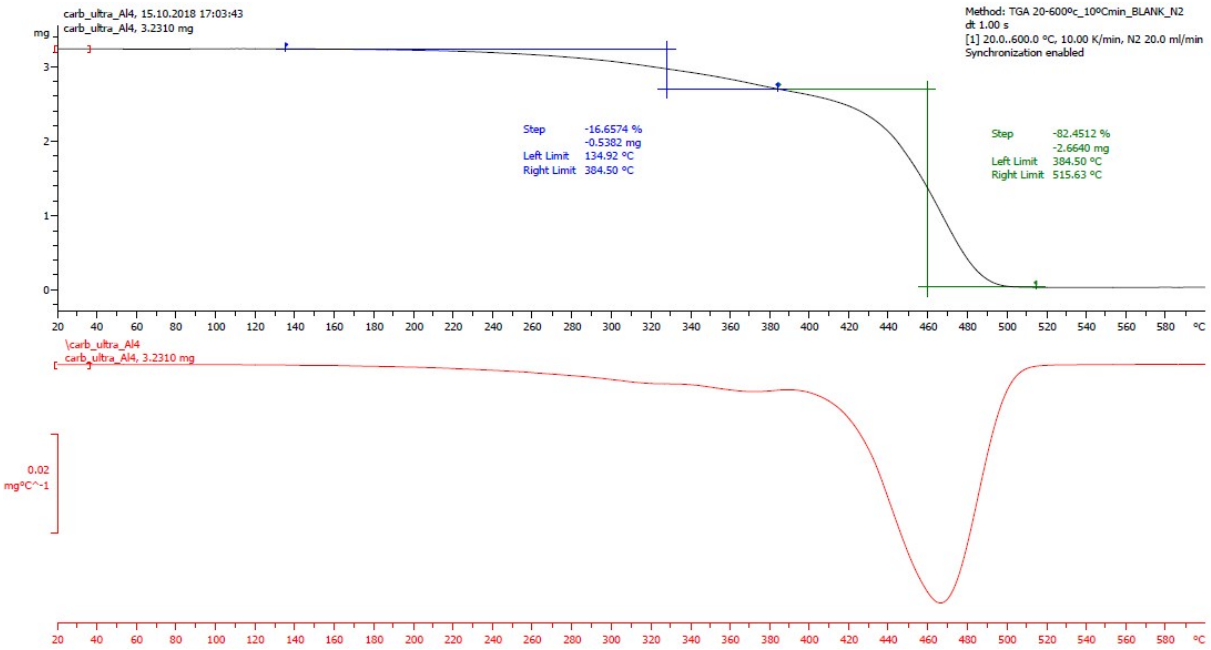

Figure S54. Thermogravimetric analysis of **PC-PBD1** (Table 2).

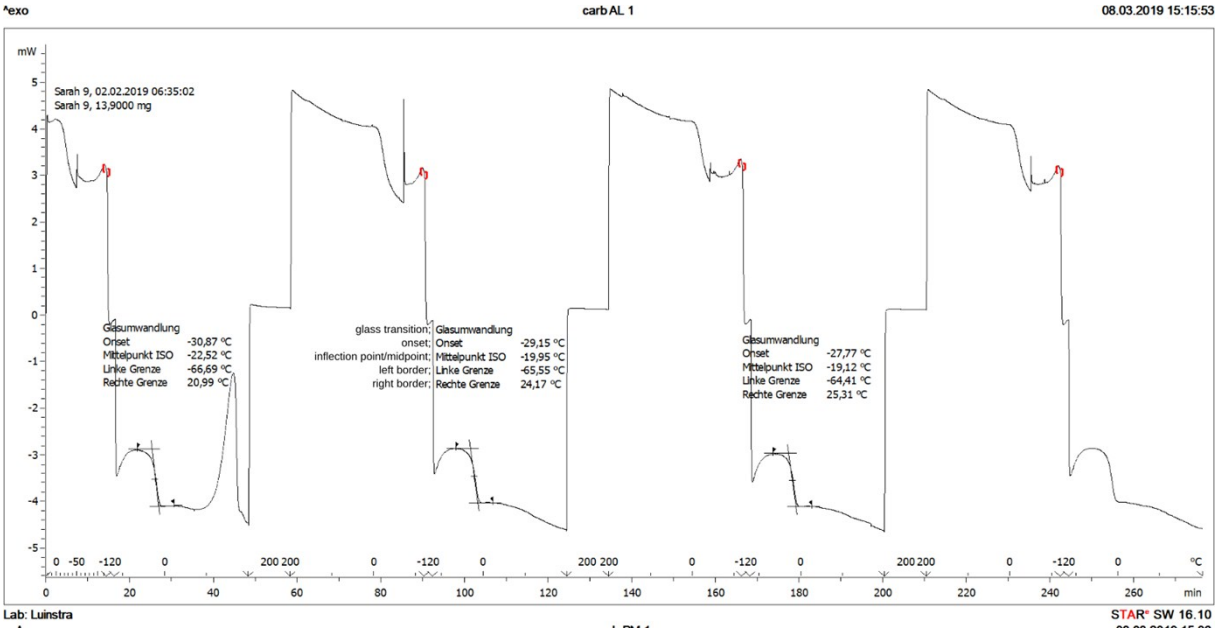

Figure S55. Differential Scanning Calorimetry trace of **PC-PBD1** (Table 2).

4.2.2 PC-PBD2

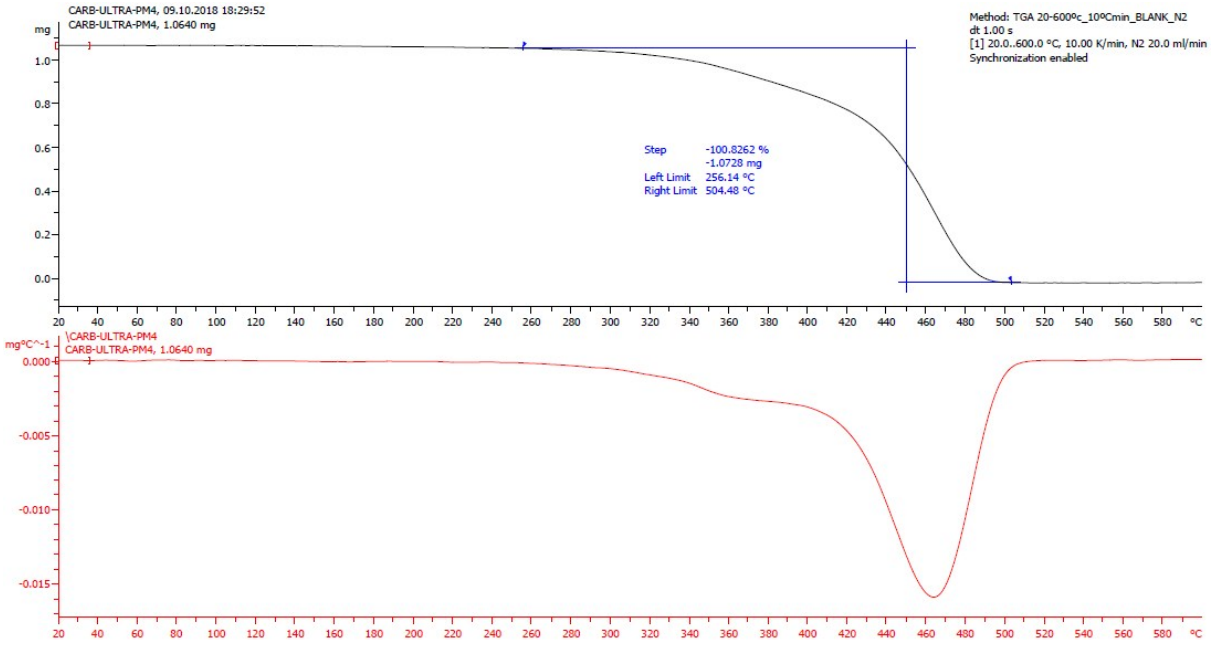

Figure S56. Thermogravimetric analysis of **PC-PBD2** (Table 2).

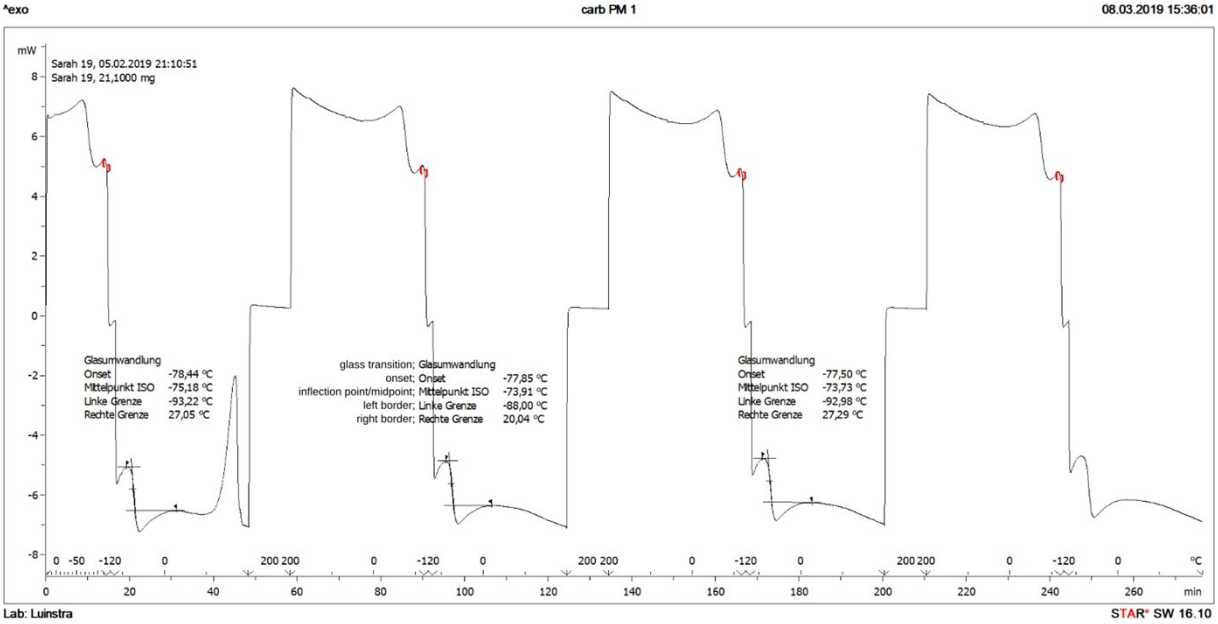

Figure S57. Differential Scanning Calorimetry trace of **PC-PBD2** (Table 2).

4.2.3 PC-PBD3

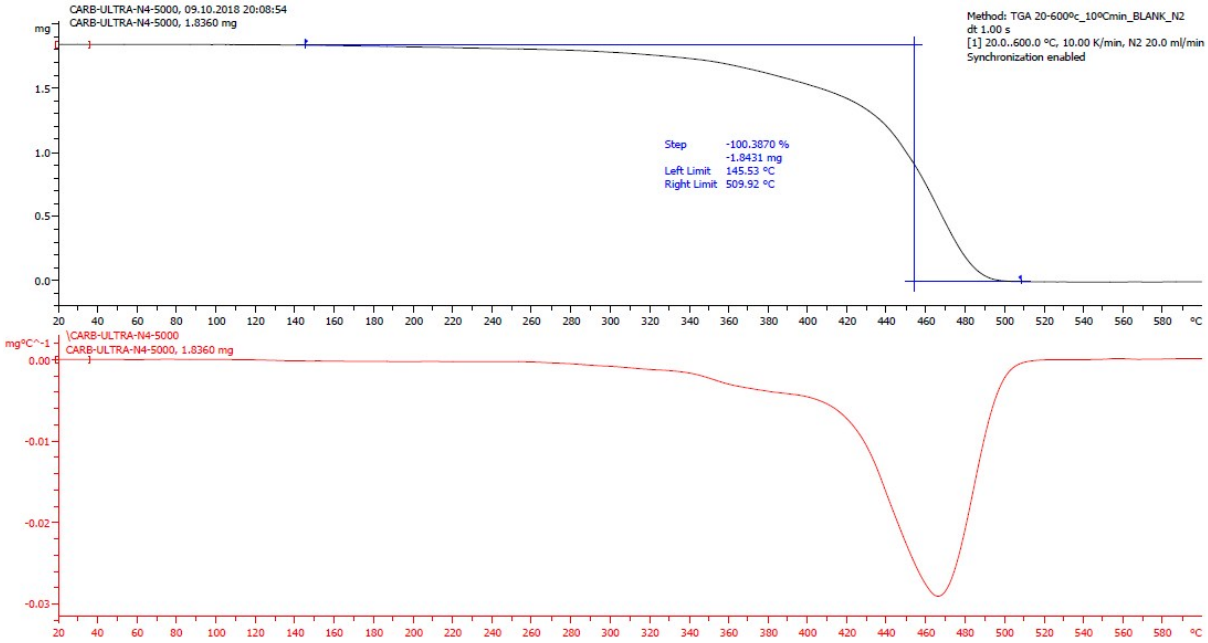

Figure S58. Thermogravimetric analysis of **PC-PBD3** (Table 2).

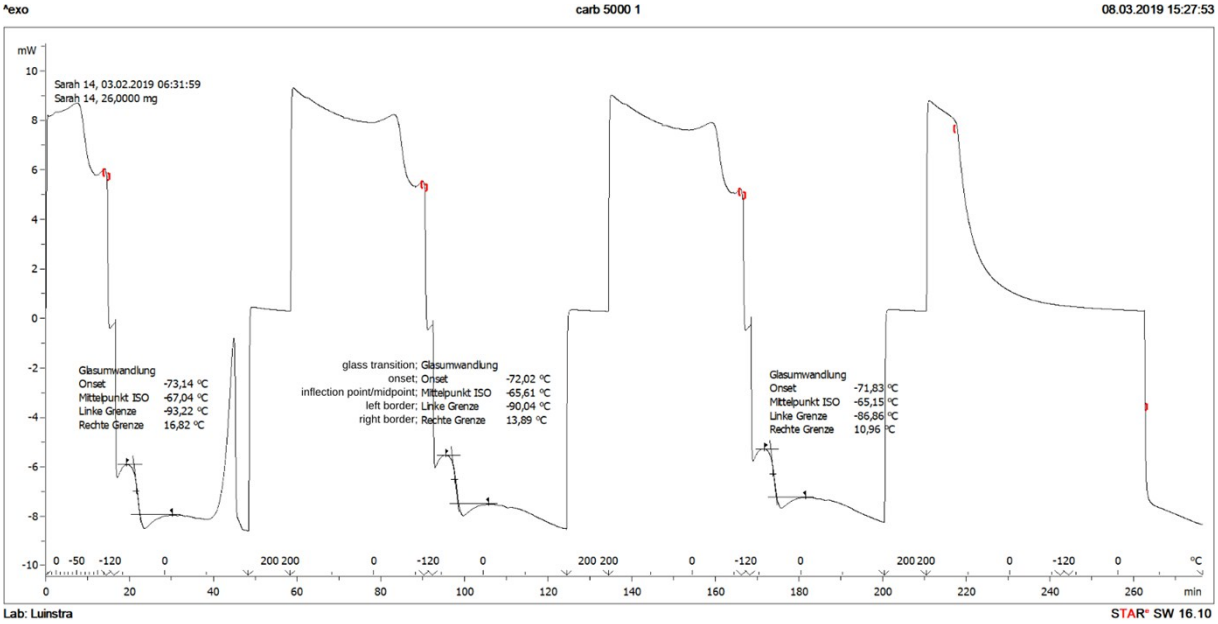

Figure S59. Differential Scanning Calorimetry trace of **PC-PBD3** (Table 2).

4.2.4 PC-PBD4

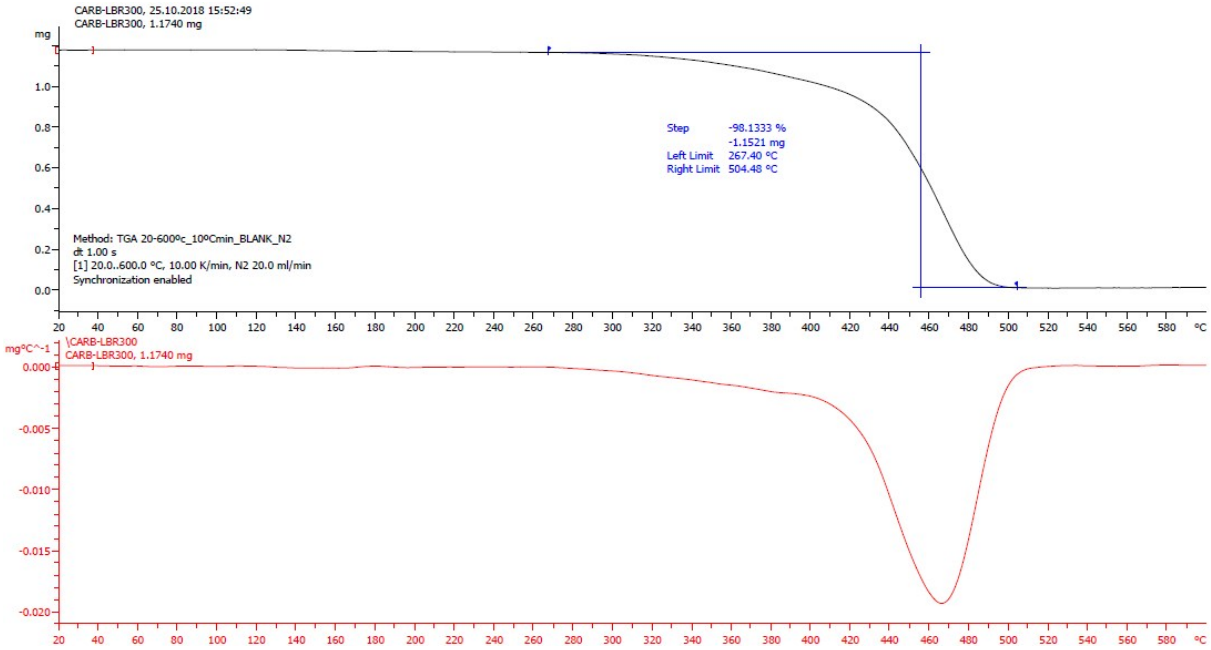

Figure S60. Thermogravimetric analysis of **PC-PBD4** (Table 2).

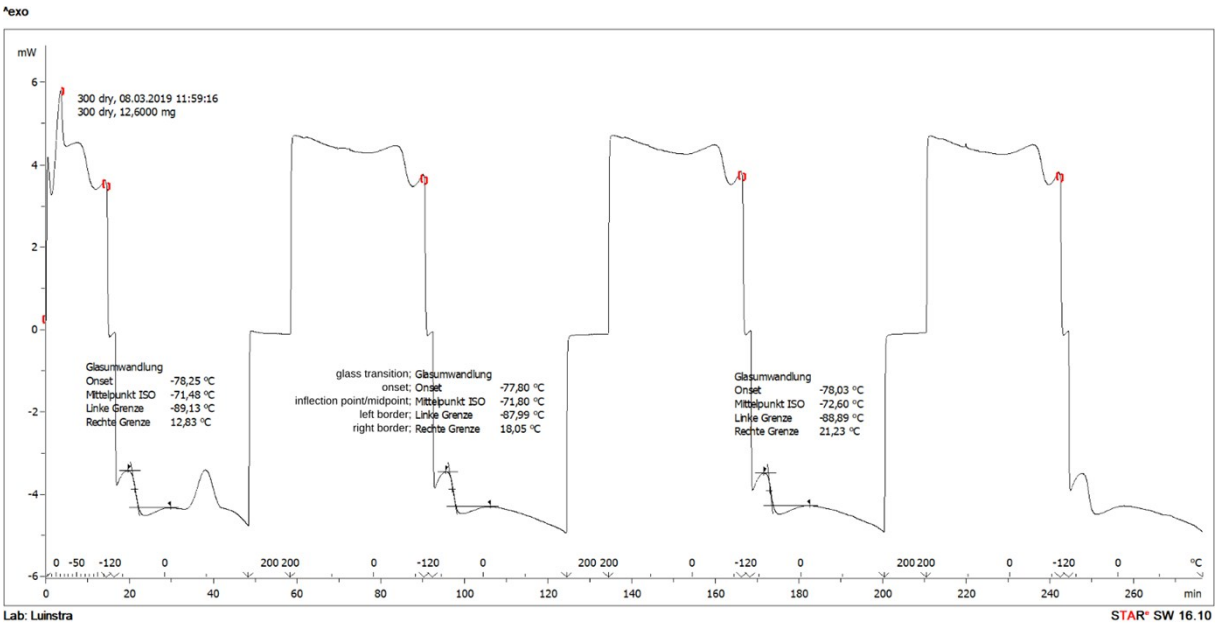

Figure S61. Differential Scanning Calorimetry trace of **PC-PBD4** (Table 2).

5. Selectivities towards the conversion of 1,2-cyclic/vinyl, 1,4-*cis* and 1,4-*trans* epoxides depending on reaction conditions demonstrated by epoxide residues in the partyl carboxylated **PE-PBDs**

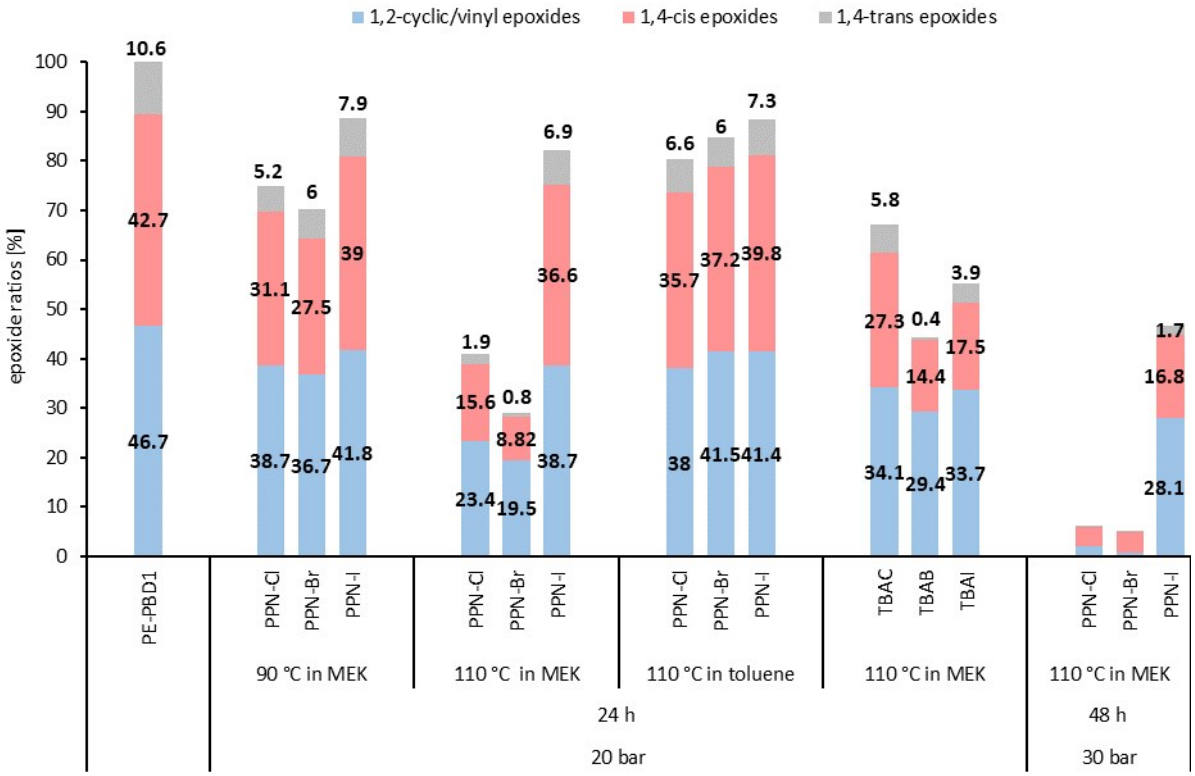

Figure S62. Epoxide ratios in partly carboxylated **PE-PBD1** after the application of different reaction conditions, solvents and reaction times.

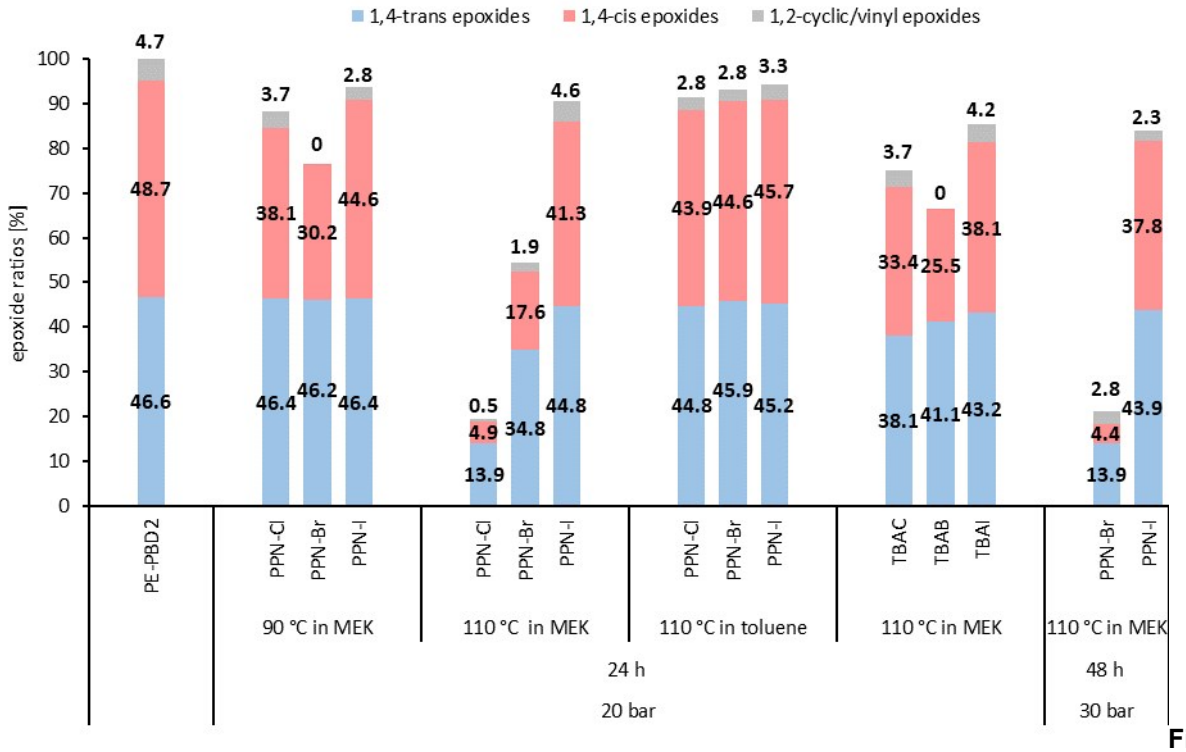

Figure S63. Epoxide ratios in partly carboxylated **PE-PBD2** after the application of different reaction conditions, solvents and reaction times.

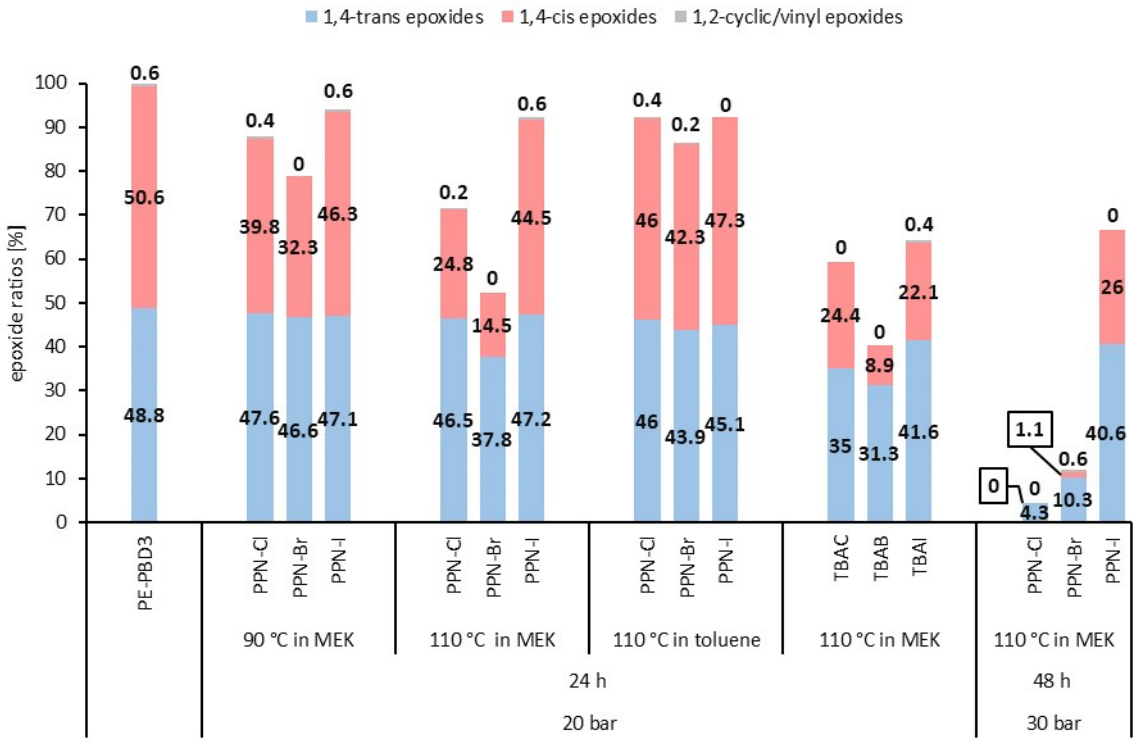

Figure S64. Epoxide ratios in partly carboxylated **PE-PBD3** after the application of different reaction conditions, solvents and reaction times.

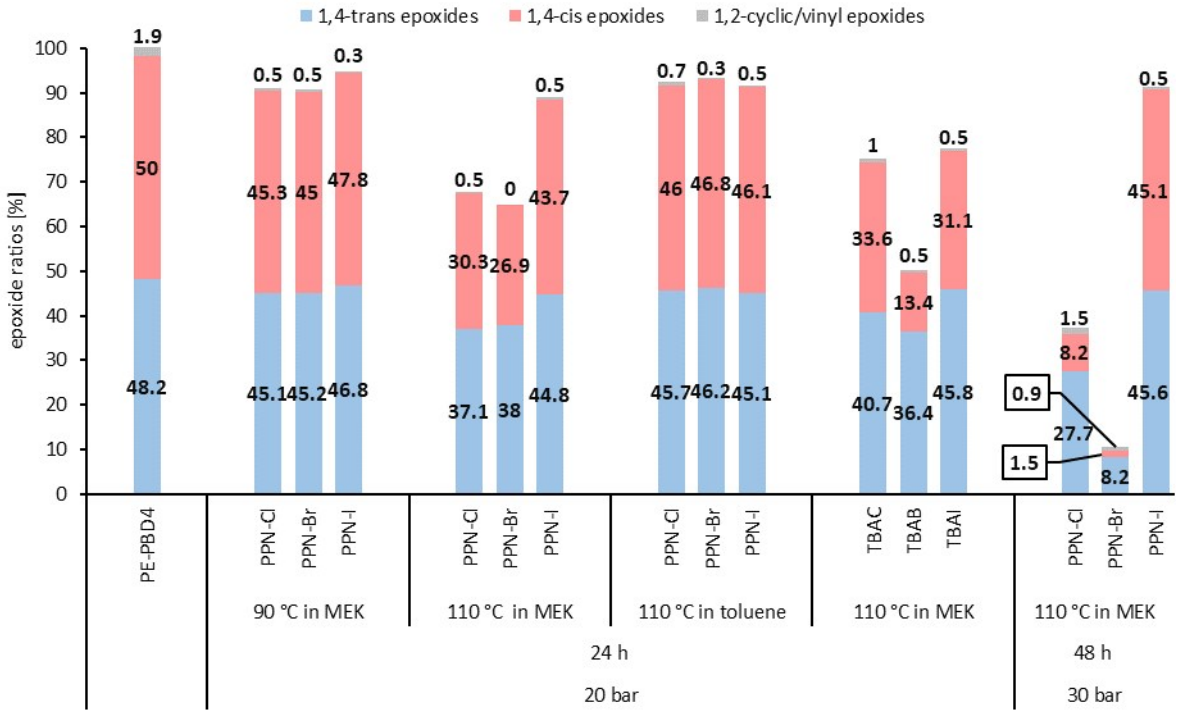

Figure S65. Epoxide ratios in partly carboxylated **PE-PBD4** after the application of different reaction conditions, solvents and reaction times.

6. GPC analysis

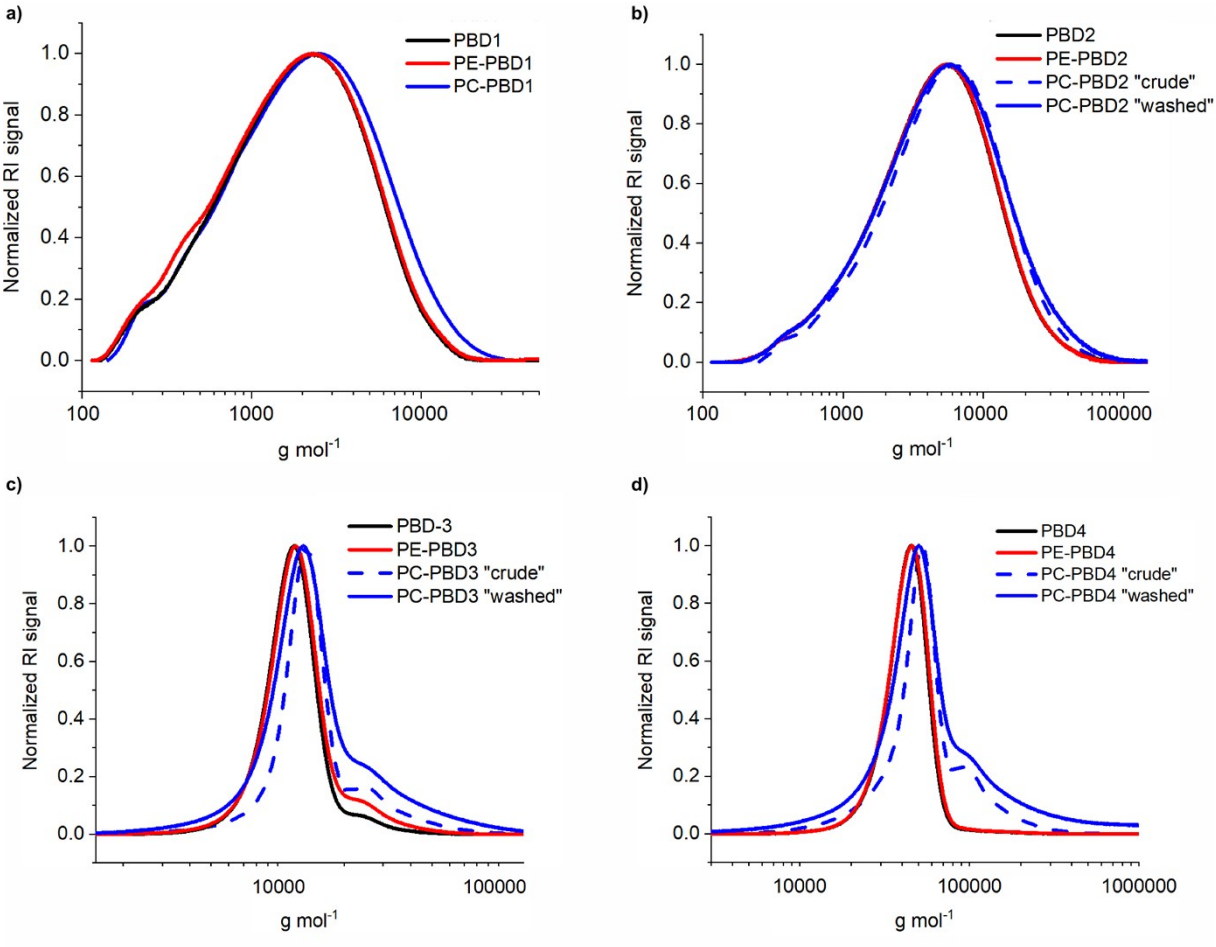

Figure S66. GPC analysis of the sequential transformation a) from **PBD1** to **PC-PBD1**, b) **PBD2** to **PC-PBD2**, c) **PBD3** to **PC-PBD3** and d) **PBD4** to **PC-PBD4**.

7. IR Characterization NIPU reactions

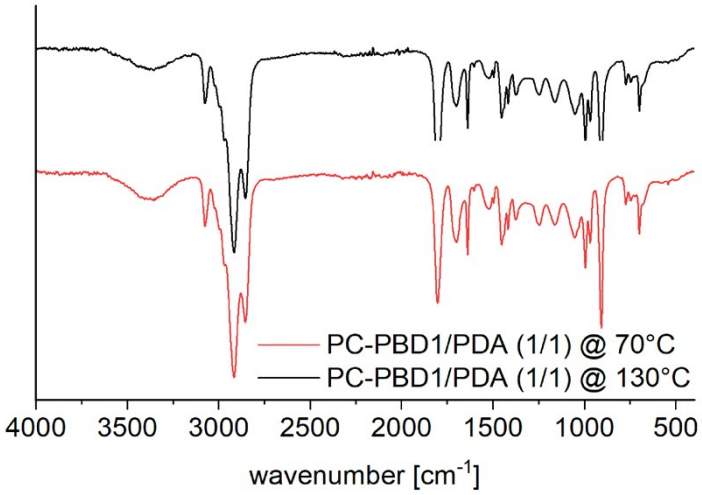

Figure S67. IR-spectra of **PC-PBD1** cured with PDA (1/1) at 70 °C and 130°C for 16h.

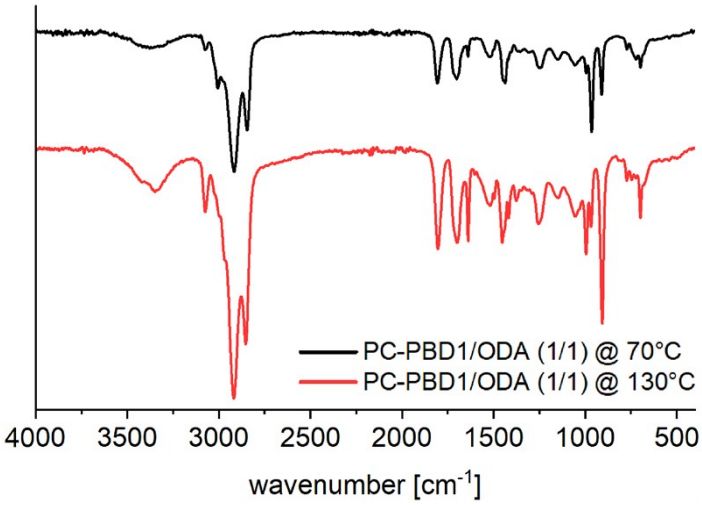

Figure S68. IR-spectra of **PC-PBD1** cured with ODA (1/1) at 70 °C and 130°C for 16h.

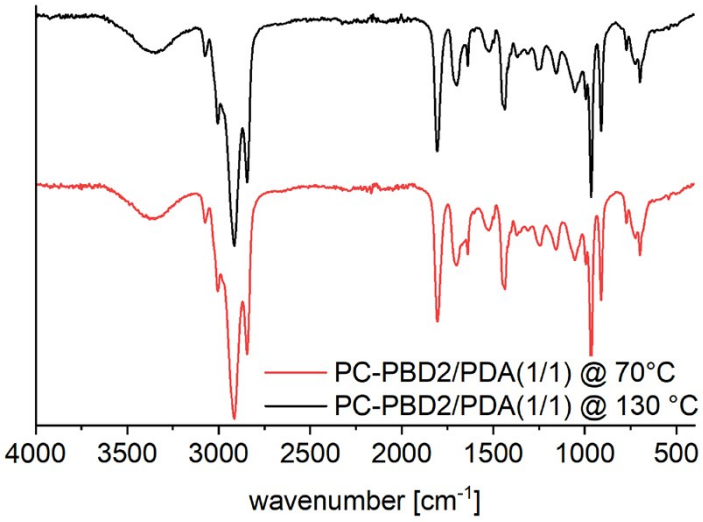

Figure S69. IR-spectra of **PC-PBD2** cured with PDA (1/1) at 70 °C and 130°C for 16h.

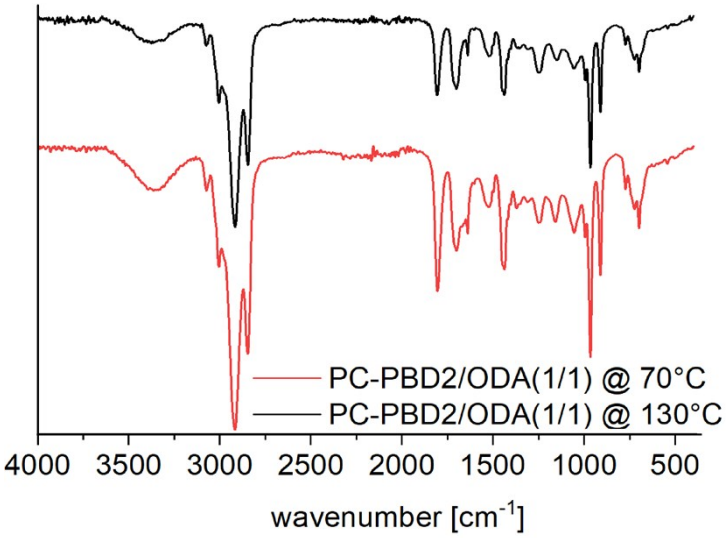

Figure S70. IR-spectra of **PC-PBD2** cured with ODA (1/1) at 70 °C and 130°C for 16h.